frontiers in Ecology and Evolution

ORIGINAL RESEARCH
published: 17 December 2020
doi: 10.3389/fevo.2020.570032

Strontium and Oxygen Isotope Analyses Reveal Late Cretaceous Shark Teeth in Iron Age Strata in the Southern Levant

Thomas Tütken[1], Michael Weber[1], Irit Zohar[2,3], Hassan Helmy[4], Nicolas Bourgon[5], Omri Lernau[3], Klaus Peter Jochum[6] and Guy Sisma-Ventura[7]**

[1] Institute of Geosciences, Johannes Gutenberg University of Mainz, Mainz, Germany, [2] Beit Margolin, Oranim Academic College, Kiryat Tivon, Israel, [3] Zinman Institute of Archaeology, University of Haifa, Haifa, Israel, [4] Department of Geology, Minia University, Minia, Egypt, [5] Max Planck Institute for Evolutionary Anthropology, Leipzig, Germany, [6] Department of Climate Geochemistry, Max Planck Institute for Chemistry, Mainz, Germany, [7] Oceanographic and Limnological Research, Haifa, Israel

Skeletal remains in archaeological strata are often assumed to be of similar ages. Here we show that combined Sr and O isotope analyses can serve as a powerful tool for assessing fish provenance and even for identifying fossil fish teeth in archaeological contexts. For this purpose, we established a reference Sr and O isotope dataset of extant fish teeth from major water bodies in the Southern Levant. Fossil shark teeth were identified within Iron Age cultural layers dating to 8–9th century BCE in the City of David, Jerusalem, although the reason for their presence remains unclear. Their enameloid $^{87}Sr/^{86}Sr$ and $\delta^{18}O_{PO4}$ values [0.7075 ± 0.0001 (1 SD, n = 7) and 19.6 ± 0.9‰ (1 SD, n = 6), respectively], are both much lower than values typical for modern marine sharks from the Mediterranean Sea [0.7092 and 22.5–24.6‰ (n = 2), respectively]. The sharks' $^{87}Sr/^{86}Sr$ are also lower than those of rain- and groundwater as well as the main soil types in central Israel (≥0.7079). This indicates that these fossil sharks incorporated Sr ($^{87}Sr/^{86}Sr \approx 0.7075$) from a marine habitat with values typical for Late Cretaceous seawater. This scenario is in line with the low shark enameloid $\delta^{18}O_{PO4}$ values reflecting tooth formation in the warm tropical seawater of the Tethys Ocean. Age estimates using $^{87}Sr/^{86}Sr$ stratigraphy place these fossil shark teeth at around 80-million-years-old. This was further supported by their taxonomy and the high dentine apatite crystallinity, low organic carbon, high U and Nd contents, characteristics that are typical for fossil specimens, and different from those of archaeological Gilthead seabream (*Sparus aurata*) teeth from the same cultural layers and another Chalcolithic site (Gilat). Chalcolithic and Iron Age seabream enameloid has seawater-like $^{87}Sr/^{86}Sr$ of 0.7091 ± 0.0001 (1 SD, n = 6), as expected for modern marine fish. Fossil shark and archaeological Gilthead seabream teeth both preserve original, distinct enameloid $^{87}Sr/^{86}Sr$ and $\delta^{18}O_{PO4}$ signatures reflecting their different aquatic habitats. Fifty percent of the analysed Gilthead seabream teeth derive from hypersaline seawater, indicating that these seabreams were exported from the hypersaline Bardawil Lagoon in Sinai (Egypt) to the Southern Levant since the Iron Age period and possibly even earlier.

Keywords: strontium isotopes, oxygen isotopes, Nile, Selachii, Teleostei, fish provenance, fossil shark teeth, enameloid

OPEN ACCESS

Edited by:
Brooke Crowley, University of Cincinnati, United States

Reviewed by:
Laszlo Kocsis, Universiti Brunei Darussalam, Brunei
Malte Willmes, University of California, Santa Cruz, United States

****Correspondence:***
Thomas Tütken
tuetken@uni-mainz.de
Guy Sisma-Ventura
guy.siv@ocean.org.il;
guysis132@gmail.com

Specialty section:
This article was submitted to Paleoecology, a section of the journal Frontiers in Ecology and Evolution

Received: *05 June 2020*
Accepted: *10 November 2020*
Published: *17 December 2020*

Citation:
Tütken T, Weber M, Zohar I, Helmy H, Bourgon N, Lernau O, Jochum KP and Sisma-Ventura G (2020) Strontium and Oxygen Isotope Analyses Reveal Late Cretaceous Shark Teeth in Iron Age Strata in the Southern Levant. Front. Ecol. Evol. 8:570032. doi: 10.3389/fevo.2020.570032

HIGHLIGHTS

- Sr and O isotope reference dataset established for modern fish from the Levant.
- Fish origin inferred from coupled $^{87}Sr/^{86}Sr$ and $\delta^{18}O_{PO4}$ analysis.
- Iron Age fish assemblage from the City of David, Jerusalem, bears fossil shark teeth.
- Late Cretaceous shark teeth identified in Iron age strata by Sr and O isotopes.

INTRODUCTION

Past fish habitats have traditionally been reconstructed based on taxonomic identification of fish remains recovered in archaeological sites (e.g., Wheeler and Jones, 1989; Zohar and Biton, 2011; Zohar, 2017). Recently, stable isotope analyses of fish bioapatite have also been used as palaeoenvironmental proxies for fish habitat and provenance (e.g., Dufour et al., 2007; Otero et al., 2011; Leuzinger et al., 2015; Sisma-Ventura et al., 2015, 2018, 2019; Fetner and Iwaszczuk, 2020). In this study, we analyse the Sr and O isotope composition of teeth from modern fish derived from different marine and freshwater bodies in the Levant to provide a reference dataset for assessing the provenance of ancient fish teeth from Chalcolithic and Iron Age cultural layers in Israel.

The Use of Strontium and Oxygen Isotopes as Provenance Proxies for Fish

The strontium isotope composition ($^{87}Sr/^{86}Sr$) of the well-preserved bioapatite of fish tooth enameloid has been widely used as a chemostratigraphic dating method for marine sediments (e.g., Ingram, 1995; Kocsis et al., 2009; Harrell et al., 2016) as a proxy to infer the palaeosalinity levels of oceanic basins and brackish water bodies (e.g., Schmitz et al., 1991, 1997; Bryant et al., 1995; Reinhardt et al., 1998; Kocsis et al., 2009), as well as for tracing past freshwater habitat use in sharks (e.g., Fischer et al., 2013) and to track their migration from the marine realm into fresh water systems (Kocsis et al., 2007, 2015). This is possible because the $^{87}Sr/^{86}Sr$ of ambient (sea)water is incorporated into the bioapatite of the teeth of Elasmobranchii (subclass of cartilaginous fish) and Teleostei (bony fish) *in vivo*, without any apparent measurable isotope fractionation (Vennemann et al., 2001). Marine fish tooth enameloid thus has a Sr isotope composition that reflects seawater $^{87}Sr/^{86}Sr$, which today is a globally constant value of 0.70918 (Hodell et al., 1990; Mokadem et al., 2015; McArthur et al., 2020), but has varied over geological time (i.e., Phanerozoic) between values of around 0.7072–0.7092 (McArthur et al., 2020). Across the last glacial-interglacial cycle the seawater $^{87}Sr/^{86}Sr$ did not deviate measurably from the modern-day value ($^{87}Sr/^{86}Sr$ = 0.7091792 ± 0.00000212 SE, n = 17; Mokadem et al., 2015). In contrast, the $^{87}Sr/^{86}Sr$ of Sr dissolved in surface freshwater bodies (rivers and lakes) depends both on the Sr isotope composition of the local bedrock (age and lithology; e.g., Goldstein and Jacobsen, 1987) and groundwater and precipitation (Herut et al., 1993; Chadwick et al., 1999; Vengosh et al., 1999) in the drainage area of rivers and lakes. Freshwater will thus have $^{87}Sr/^{86}Sr$ below or above the contemporaneous global seawater value (Dufour et al., 2007). The $^{87}Sr/^{86}Sr$ in fish teeth can be used as a proxy to distinguish between freshwater and marine habitats (**Figure 1A**; e.g., Schmitz et al., 1997; Kocsis et al., 2007, 2014; Tütken et al., 2011; Fischer et al., 2013), whereas for brackish water bodies the $^{87}Sr/^{86}Sr$ depends on the sea-to-freshwater mixing ratio (Bryant et al., 1995; Reinhardt et al., 1998).

The phosphate oxygen isotope composition ($^{18}O/^{16}O$ expressed as $\delta^{18}O_{PO4}$ value) of bony fish and shark (we refer to these collectively as 'fish' elsewhere in the paper) tooth enameloid has been used to reconstruct past seawater temperatures (e.g., Kolodny and Raab, 1988; Kolodny and Luz, 1991; Pucéat et al., 2003), seawater salinity changes (Zacke et al., 2009; Leuzinger et al., 2015) and past aquatic fish habitats such as rivers, lakes, and lagoons (Kolodny et al., 1983; Dufour et al., 2007; Klug et al., 2010; Otero et al., 2011; Kocsis et al., 2015; Leuzinger et al., 2015; Sisma-Ventura et al., 2015, 2018, 2019). Fish bones and teeth are mineralised in oxygen isotope equilibrium with their body fluids. The body fluids of fish have the same oxygen isotope composition as the ambient water ($\delta^{18}O_{Water}$) in which they reside and the body (i.e., tooth formation) temperature of fish is identical to the ambient water temperature (**Figure 1A**). Thus, the bioapatite $\delta^{18}O_{PO4}$ values of fish bones and teeth are controlled by the local $\delta^{18}O_{Water}$ value and water temperature according to the temperature-dependent water-phosphate oxygen isotope fractionation (Longinelli and Nuti, 1973; Kolodny et al., 1983; Pucéat et al., 2010; Lécuyer et al., 2013). The $\delta^{18}O_{Water}$ values of the modern oceans are ≈ 0.0‰ in tropical and subtropical regions and are more positive in evaporative basins such as the Mediterranean Sea (≈ 1.5‰), while fresh- and meltwater influx at high latitudes results in negative surface water values (between −2.0 and −4.0‰; Rohling, 2007).

The $^{87}Sr/^{86}Sr$ of rivers and lakes is controlled by dissolved Sr released from the weathering of bedrock in catchment areas (Goldstein and Jacobsen, 1987; Woodward et al., 2015). This enables us to distinguish fish from bodies of freshwater draining bedrocks of different ages and lithologies, which have distinct $^{87}Sr/^{86}Sr$ (**Figure 1A**). Brackish water, which is a mixture of seawater and freshwater, will have variable $^{87}Sr/^{86}Sr$, depending on the mixing ratio of the waters, Sr content, and the $^{87}Sr/^{86}Sr$ of the freshwater input (e.g., Bryant et al., 1995; Reinhardt et al., 1998; Hobbs et al., 2019). Brackish water is typical in estuaries of rivers and coastal wetlands.

Combined Sr and O isotope analysis of fish remains therefore represents a promising geochemical approach for assessing fish provenance in archaeological and palaeontological contexts. In this study we establish a reference dataset of Sr and O isotope values by analysing the teeth of modern fish from different water bodies in Egypt and Israel. We then use this reference dataset to reconstruct past fish habitats by analysing fish remains from Chalcolithic (Gilat) and Iron Age (City of David, Jerusalem) archaeological sites in the Southern Levant.

Fish as a Commodity

Identification of fish trade in antiquity is traditionally based on the presence of "exotic" fish remains in archaeological sites, which are distantly located from the original habitat of the fish (Davis,

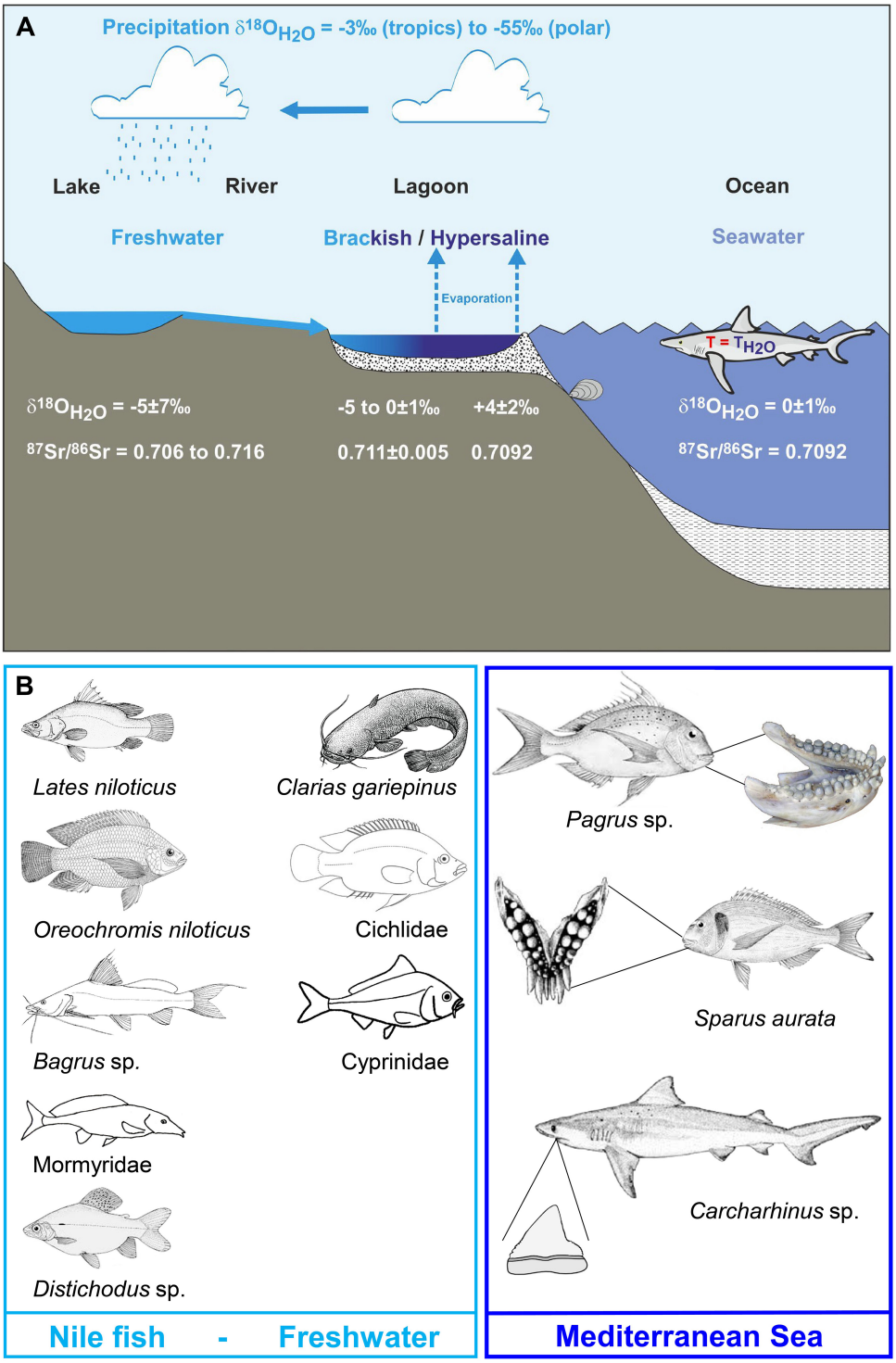

FIGURE 1 | Illustration of the environmental effects on the isotope signatures of water bodies and the fish species living in these aquatic habitats in the Southern Levant. **(A)** Schematic overview of the hydrological cycle affecting the $^{87}Sr/^{86}Sr$ and the $\delta^{18}O_{Water}$ of marine to freshwater bodies that represent typical fish habitats. The $^{87}Sr/^{86}Sr$ and $\delta^{18}O_{Water}$ values for assigning the major water bodies in Egypt and the Southern Levant to such habitat types are provided at the bottom of the figure. Note that Mediterranean seawater has a value of 1.6 ± 0.3‰ (Sisma-Ventura et al., 2016) but the same $^{87}Sr/^{86}Sr$ as global seawater. The Sr and O isotope composition of these aquatic fish habitats is controlled by the mixing of marine and freshwater which both have distinct $^{87}Sr/^{86}Sr$ and $\delta^{18}O_{Water}$ as well as by additional effects of evaporation (i.e., ^{18}O-enrichment) which only affect $\delta^{18}O_{Water}$ values. **(B)** Key freshwater and marine staple food fish (by family and species) frequently used as indicators of their habitats: Nilotic fish, Southern Levant fresh water fish, and southeast Mediterranean area (Fish belonging to Claridae, Cichlidae and Cyprinidae may represent Nilotic habitat or other freshwater habitats in the Southern Levant).

1985; Van Neer et al., 2005). In the Eastern Mediterranean region, several key species have been identified as indicators of fish trade as they occur only in one of three main aquatic habitats: the Nile (Egypt), Eastern Mediterranean and the Red Sea (**Figure 1B**). For example, Nilotic species such as *Lates niloticus* (Latidae, Nile perch), *Oreochromis niloticus* (Cichlidae; Nile tilapia), *Bagrus* sp. (Bagridae, bagrid catfish) (Van Neer et al., 1997, 2004, 2005, 2015; Van Neer and Depraetere, 2005) are considered typical indicators of fish trade from Egypt to the Southern Levant. Recently, stable isotope studies of archaeological fish teeth demonstrated that Gilthead seabream (Sparidae; *Sparus aurata*) were also exported from Egypt to this area of modern-day Israel as they derive from the hypersaline Bardawil Lagoon in northern Sinai (**Figure 2A**) and not from local fishing activity (Sisma-Ventura et al., 2015, 2018, 2019). The occurrence of imported fish in archaeological layers demonstrates that Nilotic and lagoonal fish were common trade goods from the Bronze Age onwards (Van Neer and Ervynck, 2004; Van Neer et al., 2004, 2005, 2015; Raban-Gerstel et al., 2008; Sisma-Ventura et al., 2015, 2018, 2019; Zohar and Artzy, 2019).

However, most of these studies have concentrated on bony fish, while shark (Elasmobranchii) exploitation and trade routes have received little attention. In general, Elasmobranchii (Chondrichthyes) do not preserve well because, with the exception of their teeth, dermal denticles, spines and vertebrae centra, the rest of their skeleton is composed of cartilage (Wheeler and Jones, 1989; Rick et al., 2002). Teeth and vertebrae centra are typically the main shark remains found in archaeological contexts. While shark vertebrae centra are commonly found and usually well preserved, shark teeth are rarely recovered, even when the soil is carefully sieved (**Table 1** and references therein). Interestingly, previous studies (Cione and Bonomo, 2003; Betts et al., 2012; Charpentier et al., 2020) determined that fossil shark teeth recovered from archaeological contexts have been employed as ornaments and tools, while shark vertebrae centra are only rarely identified as jewelry (Boulanger et al., 2020) and are usually interpreted as food remnants.

A review of published data on *ca.* 30,000 fish remains recovered in Holocene archaeological sites in the Southern Levant (**Table 1**) shows that 511 elasmobranch remains (sharks or rays), were recovered from 37 sites dated from the Pre-Pottery Neolithic A (*ca.* 10,000 BC) until the Crusader period (*ca.* 1099 AD). Most of the remains are vertebrae centra, and the earliest appearance of elasmobranchs occur in the Pre-Pottery Neolithic A (Sultanian) level of the inland site of Hatoula (Lernau and Lernau, 1994), and in the Pre-Pottery Neolithic C (PPNC) coastal sites of Ashkelon (Garfinkel et al., 2005; Lernau, 2008) and Atlit-Yam (Galili et al., 2004). Shark remains from the Late Chalcolithic are reported only from Namir road (Van den Brink et al., 2016) and from the Early Bronze Age layer of coastal Ashkelon Afridar (Lernau, 2004). Elasmobranch remains occur in most sites dating to the Late Bronze Age until the Crusader period, regardless of the sieving method applied. However, in all cases shark teeth are rarely recovered (8.4% of all shark remains), and out of 43 identified shark teeth, 38 (88%) were excavated in the City of David, Jerusalem (**Table 1**).

From an economic and dietary perspective, elasmobranchs (sharks and rays) are regarded as attractive food source since they are rich in protein, vitamin A, and oil. Additionally, their skin may be used as sandpaper and their spines and teeth (including

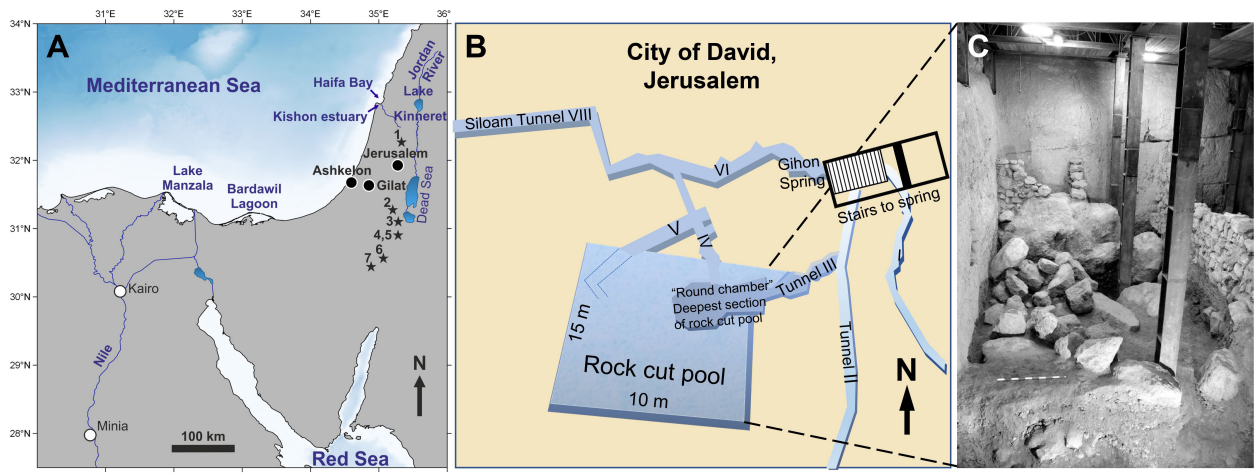

FIGURE 2 | (A) Map of the main water bodies and potential fish habitats of Egypt and the Southern Levant: Mediterranean Sea, Red Sea, upper Nile River, the brackish Lake Manzala on the Nile delta, the hypersaline Bardawil Lagoon in northern Sinai, and the freshwater Lake Kinneret and Jordan River, its main tributary, in northern Israel. These represent the key modern and past fish habitats from which we analysed modern fish samples to establish a Sr and O isotope reference dataset with which to assess the provenance of archaeological fish specimens. The ancient (i.e., fossil and historic) fish teeth were analysed from three different archaeological sites (black circles): Gilat (Chalcolithic), Ashkelon (Iron Age I), and Jerusalem/City of David (Iron Age I-II). Localities where fossil Cretaceous shark teeth were found in Israel (stars) after Kolodny and Raab (1988) and Retzler et al. (2013): **1** Ein Yabrud, **2** Letaot Mt., **3** Mishor Rotem, **4** HaMakhtesh HaKatan, **5** Ein Aqrabbim, **6** Hor Hahar, **7** Makhtesh Ramon. **(B)** Location map of the "Rock Cut Pool" adjacent to the Gihon spring, City of David, Jerusalem, and the nearby Siloam stream. **(C)** Photograph of the eastern wall of the "Rock Cut Pool" with the limestone boulders of the infill. Both **(B,C)** modified after Reich et al. (2007, 2008) and Sneh et al. (2010).

TABLE 1 | Elasmobranchii (sharks and rays) remains recovered from coastal and inland archaeological sites, by period, total number of fish remains recovered (NISP), number of cartilaginous fish, number of shark teeth and published reference.

Site	Period	Site location	Total NISP	Elasmobranchii		References
				NISP	Teeth	
Hatoula	Sultanian	Inland	110	1	0	Lernau and Lernau, 1994
Ashkelon	PPNC	Coastal	1753	19	0	Garfinkel et al., 2005
Atlit–Yam	PPNC	Coastal	3842	1	0	Zohar et al., 1994; Galili et al., 2004
Namir Road	Late Chalcolithic	Coastal	358	3	0	Van den Brink et al., 2016
Qatif	Chalcolithic	Coastal	129	14	0	Van den Brink et al., 2016
Gilat	Chalcolithic	Inland	36	3	0	Van den Brink et al., 2016
Ashkelon Afridar	EB	Coastal	54	1	0	Lernau, 2004
Tel Yoqneam	PN–IA II	Inland	192	4	1	Horwitz et al., 2005
Tel Kabri	MB IIb	Inland	2	1	0	Lernau, 2002a
Haruvit	LB	Inland	564	89	0	Van Neer et al., 2005
Tel Dor G 11–12	LB II	Coastal	356	6	0	Bartosiewicz et al., 2018
Tel Abu Hawam	LB II	Coastal	86	1	0	Zohar and Artzy, 2019
Tel Aphek	LB IIb	Coastal	4		0	Lernau, 2009
Lachish	LB III	Inland	752	70	0	Lernau and Golani, 2004
Timna	LB–IA	Inland	95	1	0	Lernau, 1988
Tel Dor D	IA–I	Coastal	755	29	0	Raban-Gerstel et al., 2008
el Ahwat	IA	Inland	88	0	0	Lernau, 2011a
Jerusalem Rock cut Pool	IA	Inland	10600	39	29	Reich et al., 2007, 2008
Tel Dor-G10	IA	Coastal	737	13	0	Bartosiewicz et al., 2018
Megido	IA	Inland	157	1	0	Lernau, 2000
Tel Dor-D	IA I–II	Coastal	209	19	0	Raban-Gerstel et al., 2008
Megido	IA	Inland	70	1	0	Lernau, 2000
Tel Dor-D	IA II	Coastal	80	5	0	Raban-Gerstel et al., 2008
Tel Harasim	IA II	Inland	18	2	0	Lernau, 2002b
Ashkelon Grid 38 and 50*	IA II–604 BC	Coastal	3890	154	4	Lernau, 2011b
Jerusalem Haophel	IA IIb	Inland	291	1	0	Horwitz and Lernau, 2018
Jerusalem Area G	586 BCE	Inland	3062	10	9	Lernau, 2015
Tel Harrasim	Persian	Inland	13	3	0	Lernau, 2002b
Tel Dor D	Persian	Coastal	179	8	0	Raban-Gerstel et al., 2008
Tel Dor D	Hellenistic	Coastal	119	2	0	Raban-Gerstel et al., 2008
City of David	Hellenistic–Byzantine	Inland	19	1	0	Reich et al., 2007; Lernau, 2015
Upper Zohar	Early Byzantine	Inland	727	1	0	Lernau, 1995
Tel Harrasim	Inland	Inland	2	1	0	Lernau, 2002b
Ceasarea Area LL	Byzantine	Coastal	137	1	0	Fradkin and Lernau, 2008
Ceasarea Area TP	Crusader	Coastal	118	2	0	Fradkin and Lernau, 2008
Ceasarea Area TP	Islamic	Coastal	166	1	0	Fradkin and Lernau, 2008
Tel Tanninim Area A2	Crusader	Coastal	648	3	0	Fradkin and Lernau, 2006

fossil teeth) can be used as raw material for tools (Borhegyi, 1961; Noe-Nygaard, 1971; Luomala, 1984; Rick et al., 2002). Therefore, despite rare preservation in archaeological sites, when recovered in cultural contexts shark teeth have been interpreted to reflect exploitation of coastal water bodies, lagoons and estuaries and shed new light on the habitat the sharks exploited and fishing practices in the past (Serena, 2005).

The Archaeological Assemblage

Large numbers of fish remains (>10,000) were recovered in the City of David, located outside and south of the southern walls of Jerusalem Old City (present day Silwan village) (Mazar, 2015). These remains were recovered from a structure located adjacent to the Gihon spring named "The Rock Cut Pool" and dated to the Iron Age II period, 8–7th century BCE (**Figure 2B**; Reich et al., 2007, 2008; De Groot and Fadida, 2011; Reich and Shukron, 2011). This large rectangular structure (15 × 10 m) cut into the limestone bedrock has straight, almost vertical rock walls, and during the Bronze Age period, prior to the operation of Siloam water Tunnel, was probably part of a complex underground water system allowing access to water during times of siege. During the end of the 9th century BCE/beginning of the 8th century BCE, it was converted to a private house. For this purpose, the pool was filled with large limestone boulders and soil (**Figure 2C**) in order to raise the floor-level by 3 m, and then sealed by the floor of the building above it. During excavation, the sediments beneath the

floor were dry and wet sieved through a 5 mm mesh. More than 10,000 fish remains, together with 6.5 tons of pottery and several hundred broken clay seals, known as "bullae" were recovered and dated to Iron Age IIB. The "bullae" were used to seal letters or packages and thus would have been broken and thrown away when the packages and letters were opened. Fish taxonomic composition included 14 families of fish, most of them (*ca.* 90%) originating from the Mediterranean Sea (mainly Sparidae and Mugilidae) as well as some from freshwater habitats (*ca.* 8.5%) including the Nile (Reich et al., 2007, 2008). Of these fish, 39 teeth and vertebrae centra belonged to Chondrichthyes fish (sharks and rays; **Table 1**). Several of these shark teeth were analysed for this study alongside *Sparus aurata* (Gilthead seabream) teeth from this site and from the Chalcolithic site of Gilat (5800–5500 BP; Rowan and Golden, 2009).

Shark Tooth Formation

Extant elasmobranchs (a subclass of cartilaginous fish that includes sharks, skates and rays) exhibit huge diversity in tooth shape. Their dentition is comprised of a large number of highly specialised single teeth that are organised in rows, and undergo continuous replacement throughout the life of the shark (**Figure 3A**; Debiais-Thibaud et al., 2007, 2015; Jernvall and Thesleff, 2012; Rasch et al., 2016; Meredith Smith et al., 2018). Tooth replacement and dentition patterns are distinctive for sharks and rays (Underwood et al., 2016; Meredith Smith et al., 2018). In sharks, only teeth in the outer row are fully upright and functional while replacement teeth lie posteriorly with their tips angled toward the rear. Tooth development and regeneration in Chondrichthyes is still poorly understood and characterised from a developmental and genetic perspective (Rasch et al., 2016). In different modern shark species, tooth replacement cycles vary and can be as rapid as 8–10 days, as in Lemon sharks (*Negaprion brevirostris*), 28 days as in Nurse sharks (*Ginglymostoma cirratum*), 38 days as in Leopard sharks (*Triakis semifasciata*) or as long as 150 days as in Sandy dogfish (*Scyliorhinus canicular*) (Moss, 1967; Reif et al., 1978; Luer et al., 1990; Botella et al., 2009 and references therein). Thus, while all sharks replace their teeth continuously, the timing of tooth formation and replacement varies depending on the species and age of the individual (younger sharks replace their teeth faster and thus more frequently).

The teeth of sharks and bony fish consist of a compact outer layer of hard, highly mineralised enameloid and an interior core of softer, less mineralised dentine (**Figure 3A**; Enault et al., 2015; Jambura et al., 2018, 2020). The tooth root is made up of porous osteodentine, a specific kind of dentine, which contains dentinal osteons and inter-osteonal tissue, and superficially resembles osteonal bone (Enault et al., 2015; Jambura et al., 2018, 2020). Enameloid is harder and has a lower solubility than hydroxylapatite characteristic of enamel, because the bioapatite often has a high fluorine content (i.e., fluorapatite; Miake et al., 1991; Suga et al., 1993; Enax et al., 2014). Thus, enameloid is highly resistant to diagenetic alteration following *post mortem* burial, even over geological time periods (Sharp et al., 2000). In Chondrichthyes, enameloid is composed of two units: a dense tissue of single crystallite enameloid (SCE), and an inner tissue of bundled crystallite enameloid (BCE) (**Figure 3A**; Enault et al., 2015). In this study, we sampled material from SCE, wherever possible, but in some cases sampled a mixture of both of these layers.

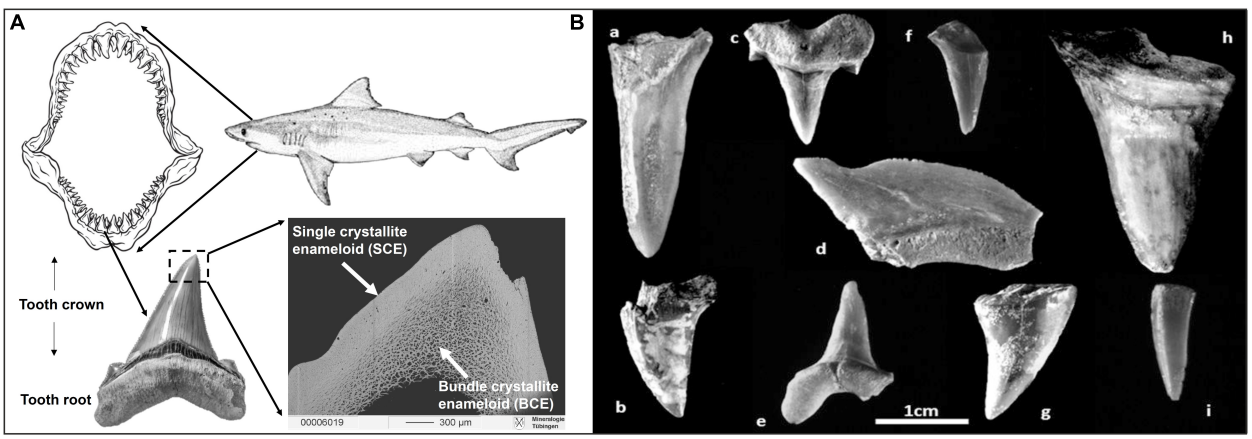

FIGURE 3 | Shark teeth illustrations. **(A)** Schematic drawing of a shark dentition with multiple rows of teeth that are continuously replaced. A photograph of a *Carcharhinus* sp. tooth is shown with the crown part covered by enameloid (consisting of fluorapatite; Enax et al., 2014) and the root part comprised of dentine (which consists of fluor-bearing hydroxylapatite). The backscattered electron image illustrates the internal enameloid microstructure of the tip of a modern Great white shark tooth showing the outer enameloid layer of single crystallites (SCE) and the inner layer of bundle crystallites (BCE). **(B)** Photographs of fossil shark teeth from the Iron Age cultural layers of the City of David from the "Rock Cut Pool" dating to the 8–9th century BCE in Jerusalem: **(a)** lamniform shark, Odontaspididae; **(b)** SK-86: shark, no taxonomic identification (NTI); **(c)** SK-79: lamniform shark, Odontaspididae, Cretaceous; **(d)** SK-85: *Squalicorax,* Late Cretaceous; **(e)** SK-84, **(f)** NTI, **(g)** SK-82, **(h)** SK-83, **(i)** SK-77: shark, NTI. Except for specimens **(a,f)**, seven of these fossil shark teeth were analysed for their Sr and O isotope composition (the unidenfied lamniform shark **(a)** and specimen **(f)** did not contain enough enameloid to sample). All of these teeth are presumably from the Late Cretaceous (**Table 2**). Note that enameloid $^{87}Sr/^{86}Sr$ of these shark teeth are fully in line with an early Campanian Sr stratigraphic age (80.29 Ma +3.24, –2.64 Ma) using the McArthur et al. (2020) dataset; **Table 2**.

MATERIALS AND METHODS

The provenance of archaeological fish remains (sharks and bony fish) recovered in the Southern Levant both from inland and coastal sites (**Figure 2**) was examined by analysing $^{87}Sr/^{86}Sr$ and $\delta^{18}O_{PO4}$ of the bioapatite of their teeth (i.e., enameloid). To assess past fish habitats and provenance we first establish a reference database of $^{87}Sr/^{86}Sr$ and $\delta^{18}O_{PO4}$ values for modern sharks as well as marine and freshwater bony fish from the major water bodies in Egypt and in the Southern Levant (Nile, Lake Kinneret, Jordan River, Bardawil Lagoon, **Figure 2A** and **Table 2**). The isotope data from archaeological fish teeth are then compared with those of modern fish to assess their origin. Additional $\delta^{18}O$ values and $^{87}Sr/^{86}Sr$ of rainwater and bedrock for each archaeological site are considered in order to infer the soil water Sr and O isotope composition and identify possible effects of *post mortem* diagenetic alteration. Additionally, the dentine apatite crystallinity, organic carbon content and trace element composition were analysed to further characterise the degree of diagenesis.

Material for Isotope Analysis

Modern Fish Tooth Samples

For O and Sr isotope analysis, we sampled teeth from bony and cartilaginous fish from different aquatic habitats in Egypt and the Southern Levant: the South-eastern Mediterranean Sea, the Nile (Minia, central Egypt), the Nile delta (Lake Manzala), the hypersaline Bardawil Lagoon (Sinai, northern Egypt), Lake Kinneret (Israel), and the Jordan River (Israel) (**Figure 2A**). Cartilaginous fish included an Eastern Mediterranean deep-sea shark (*Centrophorus granulosus;* ≈1400 m) and a Red Sea shark (*Carcharhinus plumbeus*; surface water). Bony fish included two different species of Mediterranean fish: *Conger conger* (Congridae, European Conger; deep water ≈ 1000 m) and *Sparus aurata* (Sparidae, Gilthead seabream; coastal water, Haifa Bay). From an estuarine habitat, we sampled the teeth of *Pomatomus salatrix* (Pomatomidae, blue fish; Kishon estuary, Haifa Bay). Freshwater habitats included three species of cyprinids sampled from Lake Kinneret: *Carasobarbus canis*, *Luciobarbus longiceps*, and *Capoeta damascina* (Cyprinidae). From the Nile (Egypt) we sampled four species of fish: *Lates niloticus* (Latidae; Nile perch), *Oreochromis niloticus* (Cichlidae; Nile tilapia), *Synodontis schall* (Mochokidae; upside-down catfish), and *Bagrus bajad* (Bagridae; bagrid catfish) (**Table 2**).

Archaeological Assemblage

Analysed archaeological material included six *Sparus aurata* teeth recovered from the Chalcolithic site of Gilat (Rowan and Golden, 2009; Van den Brink et al., 2016) and from the Iron Age period of the City of David (Jerusalem), as well as 10 shark teeth from the Iron Age period of the City of David, Jerusalem (Reich et al., 2007, 2008) (**Table 3** and **Figure 3B**).

Taxonomic Identification

Identification of *S. aurata* was performed using the first molariform tooth (Sisma-Ventura et al., 2019). Photos of these teeth are provided in the supplements (**Supplementary Figure S1**). Shark teeth were identified by Jürgen Kriwet from the University of Vienna. Two of these teeth were identified to the order of Lamniformes (tooth a and c in **Figure 3B**), the latter probably from the family Odontaspididae (SK-79, tooth c in **Figure 3B**), and two teeth (SK-85, tooth d in **Figure 3B** and S07815 **Supplementary Figure S1B**) were identified as *Squalicorax* an extinct taxon only occurring in the Late Cretaceous (Shimada and Cicimurri, 2005, 2006; Cappetta, 2012; Siversson et al., 2018). All identified taxa represent extinct fossil sharks belonging to the Late Cretaceous. The other shark teeth could not be identified due to poor preservation but displayed the same macroscopic appearance and preservation as the other fossil teeth (**Supplementary Figure S1**).

Isotope Analysis of Dental Tissue

Enameloid was carefully separated from the dentine by manual drilling. For *S. aurata* the cleaned tooth crown was crushed in an agate mortar after dentine removal to obtain a homogenous enameloid powder that was used for O and solution mode Sr isotope analysis. *In situ* LA-MC-ICP-MS Sr isotope analyses were performed directly on the tooth surface (in the SCE layer) of the shark teeth (**Figure 3A**). The teeth of modern Conger eel, Tilapia, Nile Perch and Gulper shark were crushed whole (due to their very small size) and analysed for Sr and O isotopes.

Screening for Diagenetic Alteration

The preservation of fish teeth excavated from the Chalcolithic and Iron Age cultural layers was determined using various analytical methods including X-ray diffraction analysis (XRD), total organic carbon (TOC) content determination, and laser ablation inductively coupled plasma mass spectrometry (LA-ICP-MS) analysis of trace elements. These analyses were performed on the dentine of the shark and Gilthead seabream teeth, as dentine is much more sensitive to diagenetic alteration than enamel(oid) (Ayliffe et al., 1994; Kohn et al., 1999; Tütken et al., 2008). Diagenesis leads to recrystallization of the bioapatite, loss of collagen (i.e., organic matter), and *post mortem* uptake of fluorine, uranium and rare earth elements (REE) (Staudigel et al., 1985; Toyoda and Tokonami, 1990; Kohn et al., 1999). Therefore, million-year-old fossil fish teeth are expected to have a much higher apatite crystallinity (i.e., larger apatite crystallite size), lower TOC and up to several orders of magnitude higher REE and U content in the dentine relative to the archaeological fish teeth (which are only a few thousand years old). In modern fish teeth, REE and U occur in very low ng/g-level concentrations (Vennemann et al., 2001; Kocsis et al., 2015; this study) - often below the detection limit of LA-ICP-MS - and are only strongly enriched in cases of *post mortem* alteration. Such mineralogical and geochemical changes enable us to clearly distinguish whether fish teeth are contemporaneous to the cultural layer being excavated, or are fossil fish teeth. For comparison, dentine from a modern Great white shark and Gilthead seabream were analysed with the same methods as unaltered reference points.

TABLE 2 | Strontium and oxygen isotope composition of modern fish teeth.

Sample ID	Family	Species	Location/Habitat	Hard tissue	$^{87}Sr/^{86}Sr$	2 SE	Type of $^{87}Sr/^{86}Sr$ Analysis	$\delta^{18}O_{PO4}$ (‰) VSMOW
Z Hai IS 1	Centrophoridae	*Centrophorus granulosus*	Mediterranean deep water	Enamel	0.70914	0.00001	S	24.6
Z Aal IS 1	Congridae	*Conger conger*	Mediterranean deep water	Enamel	0.70912	0.00001	S	24.0
K Car IS 1	Carcharhinidae	not identified	Pelagic – Mediterranean	Bone (vertebra)	0.70920	0.00005	LA	22.5
Z SP IS 1	Sparidae	*Sparus aurata*	Haifa Bay, Israel	Enamel	0.70917	0.00005	LA	23.2
				Enamel	0.70918	0.00005	LA	23.3
				Enamel	0.70921	0.00005	LA	22.5
Z Hai IS 2	Carcharhinidae	*Carcharhinus plumbeus*	Red Sea surface water	Enamel	0.70920	0.00004	LA	22.7
				Enamel	0.70918	0.00004	LA	
				Dentin	0.70919	0.00004	LA	
				Dentin	0.70917	0.00003	LA	
				Dentin	0.70915	0.00003	LA	
Z PO IS 1	Pomatomidae	*Pomatomus salatrix*	Kishon estuary, Israel	Tooth	0.70909	0.00004	LA	19.0
				Tooth	0.70908	0.00004	LA	
				Tooth	0.70893	0.00005	LA	
				Bone (jaw)	0.70895	0.00003	LA	
				Bone (jaw)	0.70901	0.00004	LA	
				Bone (jaw)	0.70898	0.00003	LA	
K BAG ÄGY 2	Bagridae	*Bagrus bajad*	Nile River, Egypt	Bone (rib)	0.70737	0.00004	LA	
				Bone (rib)	0.70729	0.00004	LA	
				Bone (rib)	0.70720	0.00005	LA	
K NI ÄGY 2	Latidae	*Lates niloticus*	Nile, from Cairo market	Bone (jaw)	0.70716	0.00005	LA	23.4
				Bone (jaw)	0.70728	0.00004	LA	
				Bone (jaw)	0.70726	0.00004	LA	
K NI ÄGY 1	Mochokidae	*Synodontis schall*	Nile River, Egypt	Bone (pectoral spine)	0.70709	0.00005	LA	24.5
				Bone (pectoral spine)	0.70698	0.00005	LA	
				Bone (pectoral spine)	0.70704	0.00005	LA	
				Bone (pectoral spine)	0.70691	0.00004	LA	
				Bone (pectoral spine)	0.70682	0.00004	LA	
				Bone (pectoral spine)	0.70683	0.00005	LA	
K NI ÄGY 3	Latidae	*Lates niloticus*	Nile River, Egypt	Bone (jaw)	0.70681	0.00002	S	20.1
Manzala 1-Z	Cichlidae	*Oreochromis niloticus*	Lake Manzala, Port Said, Egypt	Enamel	0.70828	0.00002	S	24.4
Manzala 2-Z	Cichlidae	*Oreochromis niloticus*	Lake Manzala, Port Said, Egypt	Enamel				24.2
Manzala 2-B				Bone (jaw)				22.7
Manzala 3-Z	Cichlidae	*Oreochromis niloticus*	Lake Manzala, Port Said, Egypt	Enamel				23.8
Manzala 4-Z	Cichlidae	*Oreochromis niloticus*	Lake Manzala, Port Said, Egypt	Enamel	0.70821	0.00002	S	24.0
Manzala 4-B				Bone (jaw)	0.70821	0.00001	S	22.5
Nile 1-Z	Cichlidae	*Oreochromis niloticus*	Nile, Minia, Egypt	Enamel	0.70704	0.00002	S	23.9
Nile 2-Z	Cichlidae	*Oreochromis niloticus*	Nile, Minia, Egypt	Enamel	0.70703	0.00002	S	23.3
Nile 2-B				Bone (jaw)	0.70704	0.00002	S	21.3
Nile 3-Z	Cichlidae	*Oreochromis niloticus*	Nile, Minia, Egypt	Enamel				23.2
Nile 3-B				Bone (jaw)				22.3
Nile 4-Z	Cichlidae	*Oreochromis niloticus*	Nile, Minia, Egypt	Enamel				21.7

(Continued)

TABLE 2 | Continued

Sample ID	Family	Species	Location/Habitat	Hard tissue	$^{87}Sr/^{86}Sr$	2 SE	Type of $^{87}Sr/^{86}Sr$ Analysis	$\delta^{18}O_{PO4}$ (‰) VSMOW
Nile 4-B				Bone (jaw)				23.4
Nile 5-Z	Cichlidae	*Oreochromis niloticus*	Nile, Minia, Egypt	Enamel				24.1
Z BA IS 2	Cyprinidae	*Carasobarbus canis*	Lake Kinneret/Jordan River, Israel	Enamel	0.70757	0.00008	LA	15.5
				Enamel	0.70752	0.00006	LA	
				Enamel	0.70745	0.00006	LA	
Z BA IS 1	Cyprinidae	*Luciobarbus longiceps*		Enamel	0.70731	0.00006	LA	20.1
				Enamel	0.70750	0.00006	LA	
				Enamel	0.70741	0.00006	LA	
Z CA IS 1	Cyprinidae	*Capoeta damascina*		Enamel	0.70681	0.00005	LA	13.8
				Enamel	0.70690	0.00005	LA	
				Enamel	0.70729	0.00005	LA	
K CA IS 1	Mochokidae	Not identified	Lake Kinneret/Jordan River, Israel	Bone (spine)	0.70715	0.00005	LA	17.3
				Bone (spine)	0.70696	0.00007	LA	
				Bone (spine)	0.70731	0.00004	LA	

S: solution mode $^{87}Sr/^{86}Sr$ analysis; LA: in situ MC-LA-ICP-MS $^{87}Sr/^{86}Sr$ analysis; Note if the sample ID number is the same but a different letter at the end then B: bone and Z: enameloid are from the same fish.

TABLE 3 | Strontium and oxygen isotope composition of archaeological and fossil fish teeth.

Sample	Hard tissue	Species	Archaeological site	Age	$^{87}Sr/^{86}Sr$	2 SE	Age (Ma)[a]	$\delta^{18}O_{PO4}$ (‰) VSMOW
SP-13	Enameloid	*Sparus aurata*	City of David	Iron Age II	0.70925	0.00005		24.5*
	Bone	*Sparus aurata*			0.70875	0.00004		22.9*
SP-11	Enameloid	*Sparus aurata*	City of David	Iron Age II	0.70906	0.00006		24.2*
EB-1	Enameloid	*Sparus aurata*	Gilat	Chalcolithic	0.70916	0.00005		23.4*
EB-3	Enameloid	*Sparus aurata*	Gilat	Chalcolithic	0.70914	0.00006		23.7*
	Dentine	*Sparus aurata*			0.70902	0.00006		
EB-2	Enameloid	*Sparus aurata*	Gilat	Chalcolithic	0.70909	0.00006		22.4*
	Dentine	*Sparus aurata*			0.70867	0.00013		
EB-5	Enameloid	*Sparus aurata*	Gilat	Chalcolithic	0.70910	0.00005		24.6*
	Dentine	*Sparus aurata*			0.70918	0.00005		
SK-85	Enameloid	*Squalicorax* sp.	Jerusalem G	Late Cretaceous	0.70755	0.00006	78.23	20.0
SK-32	Enameloid	Shark NTI						20.7
SK-82	Enameloid	Shark NTI		Late Cretaceous	0.70750	0.00005	80.66	20.0
	Dentine	Shark NTI		Late Cretaceous	0.70761	0.00005		
SK-77	Enameloid	Shark NTI	Jerusalem P	Late Cretaceous	0.70760	0.00004	76.29	20.4
SK-86	Enameloid	Shark NTI		Late Cretaceous	0.70740	0.00005	86.47	20.3
SK-80	Enameloid	Shark NTI						20.2
SK-83	Enameloid	Shark NTI		Late Cretaceous	0.70750	0.00003	80.66	18.3
SK-84	Enameloid	Shark NTI		Late Cretaceous	0.70751	0.00002	80.15	
SK-79	Enameloid	Lamniform shark		Late Cretaceous	0.70752	0.00005	79.61	18.8
	Dentine			Late Cretaceous	0.70772	0.00004		
SK-76	Enameloid	Shark NTI						20.4
LN-36	Bone	*Lates niloticus*	Ashkelon	Iron Age I	0.70892	0.00006		21.0

**$\delta^{18}O_{PO4}$ data from Sisma-Ventura et al. (2018). NTI: No taxonomic identification.*
[a]*Strontium stratigraphic age in millions of years (Ma) based on the seawater $^{87}Sr/^{86}Sr$ data of McArthur et al. (2020).*

X-Ray Diffraction (XRD) Analysis

Dentine powder samples were placed on a monocrystalline, background-free silicon sample holder and X-ray diffraction patterns were analysed using a Seifert XRD 3000 TT diffractometer using a Cu cathode at 40 kV and 30 mA and Cu K_α radiation of 0.15406 nm with 0.03° (2Θ) steps in 2 s over the range from 5° to 70° 2Θ at the Institute of Geosciences, University of Mainz.

Total Organic Carbon (TOC) Analysis

The TOC content was determined in two steps. First, by analysing the dentine powders (about 10–15 mg/per sample) for total carbon (TC) content using a CN-analyser (Vario EL Cube, Elementar GmbH, Hanau, Germany) at the Institute for Geography, University of Mainz. Then, the structurally bound carbonate total inorganic carbon content (TIC) of dentine was measured using a Gasbench II coupled to a Delta V continuous flow isotope ratio gas mass spectrometer at the Max Planck Institute for Chemistry, Mainz. An internal modern elephant (*Loxodonta africana*) enamel standard (AG-Lox) of known TIC content (7.5 wt.%; Wacker et al., 2016) was analysed in different amounts to establish a regression between TIC and peak area of the mass-44 CO_2 peak. The dentine TOC content was then calculated as the difference between the TC and TIC content.

LA-ICP-MS Analysis of Trace Elements

Shark and Gilthead seabream teeth were embedded in epoxy resin to produce polished one-inch mounts. To determine the trace element compositions of enameloid and dentine, line scans were measured across the teeth (including both enameloid and dentine) by laser ablation (**Supplementary Figure S2**). The trace element measurements were performed using an ArF Excimer laser system (193 nm wavelength, NWR193 by ESI/NewWave) equipped with a TwoVol2 ablation cell and coupled to an Agilent 7500ce quadrupole ICP-MS at the Institute of Geoscience, Mainz. Laser repetition rate was set to 10 Hz with a transition speed of 10 μm/s, using a fluence of 3.5 J/cm^2. Line scans were carried out with a rectangular spot size of 130 μm × 30 μm. Pre-ablation was performed prior to each analysis to clean the surface. Background signals were acquired for 15 s during laser warm-up prior to each scan. ^{43}Ca was used as internal standard and NIST SRM 612 was used for calibration, using the preferred values from the GeoReM Database (Jochum et al., 2005). NIST SRM 610, NIST SRM 1400 and NIST SRM 1486 were used as quality control materials to test accuracy and reproducibility of the measurements (**Supplementary Table S1**). All reference materials were measured prior to and after each sample block.

Strontium Isotope (^{87}Sr/^{86}Sr) Analysis of Fish Teeth

Sr isotope analyses of all teeth were performed either by solution-based or LA-MC-ICP-MS (laser ablation inductively coupled plasma mass spectrometry) using a Nu Plasma MC-ICP-MS (Nu Instruments^{TM}) at the Max Planck Institute for Chemistry, Mainz, following the methods described by Weber et al. (2017). For solution-based analysis, the MC-ICP-MS was coupled to a CETAC Aridus 2 desolvator nebulizer system and samples were diluted to ≈ 100 ng/g Sr. A standard-sample bracketing approach was applied, using a static multi-collection mode with 100 cycles and 5 s integration time. All measurements were corrected using NIST SRM 987 (^{87}Sr/^{86}Sr of 0.710248; McArthur et al., 2020). Prior to analysis, Sr was separated by ion-exchange chromatography using Sr spec resin, following the protocol presented in Weber et al. (2018). For *in situ* laser ablation analysis, the MC-ICP-MS was coupled to a 213 nm Nd:YAG laser ablation system (New Wave Research^{TM} UP-213). Signals of the following masses were monitored during the analysis: ^{82}Kr, ^{83}Kr, ^{84}Sr, ^{85}Rb, ^{86}Sr, ^{87}Sr, ^{88}Sr and half masses 85.5 and 86.5 (half masses were only monitored during LA-MC-ICP-MS). Mass bias correction was performed using the exponential law (Ingle et al., 2003) and assuming a constant ^{86}Sr/^{88}Sr of 0.1194. Laser ablation analysis was performed by linescan analysis, each linescan with a length of 1000 μm, a circular spot size of 65–100 μm (depending on the sample and daily tuning parameter), a transition rate of 5 μm/s and a laser repetition rate of 10 Hz. The resulting fluence varied between 10–30 J/cm^2, depending on the chosen energy output (70–100%). Prior to each analysis, a pre-ablation was performed to prevent surface contamination.

To correct for Kr in the plasma, we used the "on peak zero" method by measuring a 45 s gas background prior to each analysis without the laser firing. After background subtraction, the remaining signal on mass 82 was used to check for Ca argide and dimer formation (<0.1 mV). Half masses were checked for doubly charged rare earth elements (Yb and Er) and the signals were corrected using constant isotope ratios (Berglund and Wieser, 2011). To correct for the occurrence of ^{87}Rb on mass 87, we used a ^{87}Rb/^{85}Rb of 0.3857 (Berglund and Wieser, 2011).

Samples for LA-MC-ICP-MS were measured in a standard-bracketing approach, as has been recommended as the calibration strategy for *in situ* Sr isotope analysis (Irrgeher et al., 2016; Weber et al., 2017), using the same laser parameters for both the reference material and the samples. An in-house marine shark tooth was used as reference material, assuming a modern-day ocean seawater ^{87}Sr/^{86}Sr of 0.70918 ± 0.00001. This is in the range of the modern day sea water value (Hodell et al., 1990; Mokadem et al., 2015; McArthur et al., 2020) and modern-day marine organisms (e.g., marine carbonate reference materials JCt-1 (giant clam, *Tridacna gigas*) and JCp-1 (coral, *Porites* sp.), yielding ^{87}Sr/^{86}Sr of 0.709169 ± 0.000009 (2 SE, n = 3) and 0.709170 ± 0.000006 (2 SE, n = 3, Weber et al., 2018), respectively, and modern shark samples averaging ^{87}Sr/^{86}Sr of 0.709167 ± 0.000009 (2 SE, n = 10, Vennemann et al., 2001).

Phosphate Oxygen Isotope ($\delta^{18}O_{PO4}$) Analysis of Fish Tooth Enameloid

The phosphate fraction of the fish tooth enameloid was separated using a method modified after Dettmann et al. (2001) and described in detail by Tütken et al. (2006). In summary, approximately 5 mg of pretreated sample powder was digested in 0.8 ml HF (2 M) on a vibrating table for *ca.* 12 h. After centrifugation (3 min at 10,000 rpm), the supernatant sample solution was separated from the CaF precipitates into a new

vial. After neutralising the HF solution with NH_4OH (25%) in the presence of bromothymol blue as pH indicator, Ag_3PO_4 was precipitated by adding 0.8 ml of 2 M $AgNO_3$. After settling of the Ag_3PO_4 crystals, the samples were centrifuged and the supernatant solution containing excess $AgNO_3$ was removed by pipette. The Ag_3PO_4 precipitate was then rinsed five times with Milli-Q water and dried overnight in an oven at 50°C.

Ag_3PO_4 aliquots of 0.5 mg were placed into silver capsules and analysed in triplicate by means of high temperature reduction using a Finnigan TC-EA coupled via a Conflo III to a Micromass 100 GC-IRMS at the University of Mainz, or to a Finnigan Delta Plus XL GC-IRMS at the Universities of Tübingen and Lausanne, according to the method of Vennemann et al. (2002). The raw $\delta^{18}O_{PO4}$ values were normalised to an Ag_3PO_4 reference material produced by Elemental Microanalysis with a certified value of 21.7‰ (silver phosphate P/N IVA33802207, batch no. 180097, distributed by IVA Analysentechnik, Germany). The analytical precision for this reference material was better than ± 0.3‰ (1 SD). For untreated NIST SRM 120c Florida phosphate rock, we obtained a $\delta^{18}O_{PO4}$ value of 21.9 ± 0.3‰ (1 SD, n = 15). This value compares well with the values from most other laboratories as compiled in Chenery et al. (2010).

Bioapatite $\delta^{18}O_{PO4}$ Value Reconstruction for Fish From Levantine Water Bodies

The expected isotope equilibrium range of $\delta^{18}O_{PO4}$ values for fish tooth bioapatite was calculated for each of the water bodies in Egypt and Israel from which fish were sampled using published and a few measured $\delta^{18}O_{H2O}$ values (**Table 4**). The calculations are based on the temperature-dependent isotope fractionation during biomineralisation of apatite by Lécuyer et al. (2013): T°C = 117.4 – 4.5 ($\delta^{18}O_{PO4}$ - $\delta^{18}O_{Water}$), where $\delta^{18}O_{PO4}$ and $\delta^{18}O_{Water}$ correspond to the isotope compositions of bioapatite and ambient water relative to VSMOW, respectively. This relationship is valid for the temperature range of 8°C < T < 32°C thus covering water temperatures typically encountered in the Mediterranean region. For Mediterranean surface water, we used a $\delta^{18}O_{Water}$ of 1.6 ± 0.3‰ and an annual temperature range of 17–30°C (Sisma-Ventura et al., 2014). The estimated $\delta^{18}O_{PO4}$ of Mediterranean deep water was calculated for a temperature range of 13–15°C and a $\delta^{18}O_{Water}$ value of 1.5 ± 0.2‰ (Sisma-Ventura et al., 2016). For the Nile delta water bodies, we used the post-Aswan dam $\delta^{18}O_{Water}$ range between 0.0 and 3.0‰ (Nile near Minia) and between 2.0 and 5.0‰ (Lake Manzala) and a water temperature range between 18 to 30°C (Kolodny et al., 1983; Aly et al., 2004). For Lake Kinneret and its main tributary, the Jordan River, we used a $\delta^{18}O_{Water}$ range between −6.0 and 2.0‰ and between −8.0 and −5.0‰ and a temperature range between 16–28°C and 10–22°C, respectively (Stiller and Magaritz, 1974; Talbot, 1990; Zohary et al., 1994). We also estimated the $\delta^{18}O_{PO4}$ equilibrium range of fish from past Nile delta water bodies during the Iron Age, the New Kingdom period, by using the Nile $\delta^{18}O_{Water}$ range of −2.0 to −1.0‰, reconstructed from the $\delta^{18}O_{PO4}$ values of tooth enamel from human mummies (Touzeau et al., 2013) and assuming a temperature range similar to today.

The $^{87}Sr/^{86}Sr$ and $\delta^{18}O_{PO4}$ Expectation Fields for Levantine Fish Habitats

For each of the major water bodies in Egypt and the Southern Levant we also compiled a range of expected $^{87}Sr/^{86}Sr$ water

TABLE 4 | Strontium and oxygen isotope composition of different water bodies and Sr sources in the SE Mediterranean area.

Water body/Substrate	$^{87}Sr/^{86}Sr$ range	$^{87}Sr/^{86}Sr$ mean (±1 SD)	References	$\delta^{18}O$ (‰) VSMOW range	$\delta^{18}O$ (‰) VSMOW mean (±1 SD)	References
Mediterranean seawater		0.70918	4, 6	1.3 – 1.9	1.6 (±0.3)	10
Bardawil Lagoon		0.70916	This study	1.8 – 7.2	3.7 (±2.0)	9, 14, this study
Nile (Minia, Egypt, 2019)		0.70718	This study		3.3	this study
Nile (Minia, Egypt, 1996)		0.70690	13		2.4	8
Nile (modern)	0.7060 – 0.7072		7, 13	1.0 – 2.0	1.5 (±0.5)	8, 15
Nile (New Kingdom)	0.7052 – 0.7061		5	−3.0 – 0.0	−1.4 (±1.0)	8
Lake Manzala	0.7068 – 0.7088		5, 6	3.0 – 7.0	3.5 (±1.5)	6, 14
Lake Manzala (2019)		0.70843	This study		5.0	This study
Lake Kinneret		0.70750 (±0.00005)	2	−2.5 – 0.0		12
Jordan River		0.70678 (±0.00006)	2	−6.0 to −7.0	−6.5 (±0.5)	12
Rainfall in Israel	0.7079 – 0.7092	0.7087 (±0.0004)	1	−2.0 to −8.0	−5.0 (±3.0)	11
Saharan dust		0.7078	1			
Seashore sand	0.7090 – 0.7092		3			
Calcareous sandstone		0.7090 (±0.0002)	3			
Terra rossa soils		0.70857 (±0.00026)	3			
Rendzina soils	0.7079 – 0.7084		3			

Strontium isotope data from 1: Herut et al. (1993); 2: Fruchter et al. (2017); 3: Hartman and Richards (2014); 4: McArthur et al. (2020); 5: Woodward et al. (2015); 6: Reinhardt et al. (2001); 7: Brass (1976); 8: Touzeau et al. (2013); 9: Kolodny et al. (1983); 10: Sisma-Ventura et al. (2016); 11: Gat and Dansgaard (1972); 12: Gat (1970); 13: Gerstenberger et al. (1997); 14: Aly et al. (2004); 15: Schilman et al. (2001); water samples in this study were taken in January 2019 at the following geographic coordinates: Nile (28 06 22 03 N; 30 45 17 58 E); Lake Manzala (31 16 12 82 N; 31 12 39 28 E); Bardawil Lagoon (31 03 14 32 N; 33 09 28 01 E).

values based on literature values (**Table 4**). For this purpose, we used the $^{87}Sr/^{86}Sr$ value of modern seawater of 0.70918 (Mokadem et al., 2015; McArthur et al., 2020) for the Mediterranean (including the Bardawil Lagoon) and the Red Sea. For the Nile a $^{87}Sr/^{86}Sr$ range of 0.70680–0.70718 (Minia, central Egypt, Gerstenberger et al., 1997 and this study) and for the Nile delta and Lake Manzala a range of 0.70680–0.70880 (Reinhardt et al., 2001; Woodward et al., 2015) were used. For Lake Kinneret and the Jordan River, we used a $^{87}Sr/^{86}Sr$ range of 0.70684–0.70755 (Fruchter et al., 2017). For Late Cretaceous seawater we used the $^{87}Sr/^{86}Sr$ range of 0.70728–0.70783 (for the Campanian: 0.70746–0.70774) from the $^{87}Sr/^{86}Sr$ seawater curve LOWESS 6 Fit of McArthur et al. (2020) (**Figure 4**). These $^{87}Sr/^{86}Sr$ ranges were then combined with the calculated $\delta^{18}O_{PO4}$ equilibrium ranges based on published $\delta^{18}O_{Water}$ and water temperature values to characterise each water body isotopically, and to define expected $^{87}Sr/^{86}Sr$ versus $\delta^{18}O_{PO4}$ fields for the different potential past and present main fish habitats. For fish that formed their bioapatite in Late Cretaceous seawater, we used $\delta^{18}O_{PO4}$ values ranging between 17.2 and 20.3‰ (Campanian: 18.3–20.0‰) measured in fossil shark teeth in the Southern Levant by Kolodny and Raab (1988). This reference dataset was then used as an interpretive framework to assess the provenance of the archaeological *S. aurata* and sharks based on their enameloid Sr and O isotope composition using Linear Discriminant Analysis (LDA).

Linear Discriminant Analysis (LDA)

For assessing the fish provenance from different waterbodies, we applied a LDA, a commonly used supervised pattern data-reduction and recognition method that assigns new observations to certain classes. This is achieved through a linear discriminant function (LDF) that maximises ratios of between-group variance and within-group variance. We used LDA (R package MASS version 7.3-51.6, Ripley, 2002) in order to assign provenance to archaeological fish tooth samples based on their enameloid Sr and O isotope composition. The $^{87}Sr/^{86}Sr$ ratios and $\delta^{18}O_{PO4}$ values from published and measured water samples of known provenance and associated modern fish bioapatite (bone, dentine, enameloid) samples were used as predictors. Note that the expected fish bioapatite $\delta^{18}O_{PO4}$ values for each waterbody were calculated from the $\delta^{18}O_{H2O}$ values and water temperatures using the phosphate-water oxygen isotope fractionation equation of Lécuyer et al. (2013).

In order to compute the LDF, a total of 82 observations from six different water bodies in the Southern Levant (Bardawil Lagoon, Lake Manzala, Nile River, Lake Kinneret/Jordan River, and modern Mediterranean seawater) were used. These comprise 44 observations from water samples (using min, max and mean

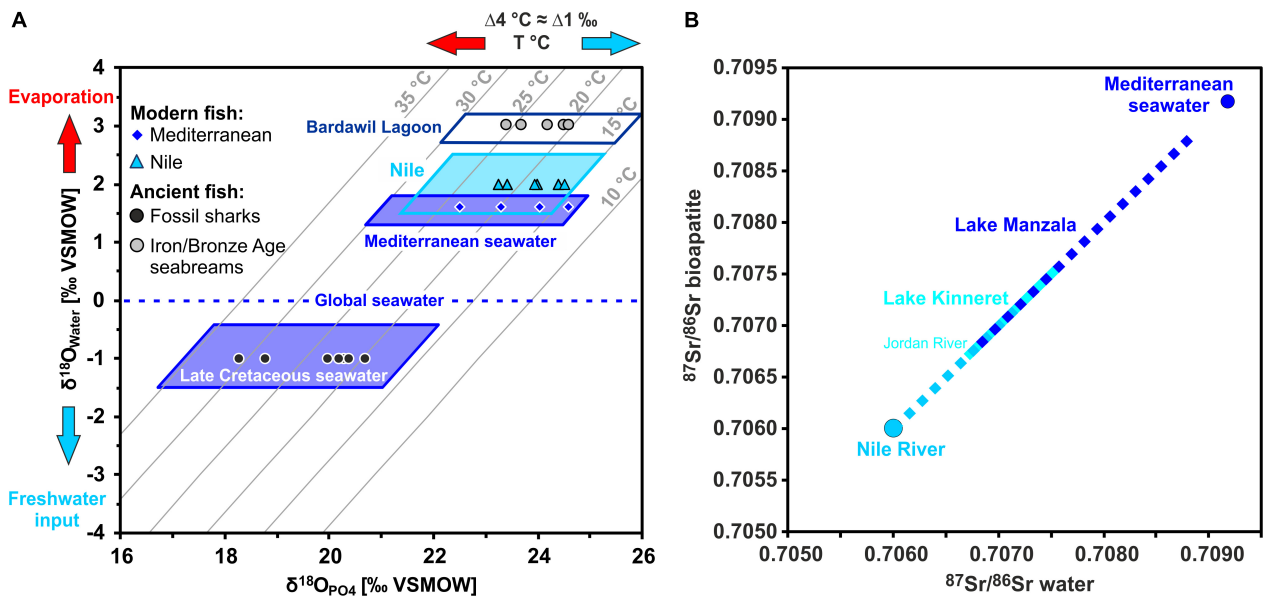

FIGURE 4 | Strontium and oxygen isotope compositions of fish teeth and their expected isotopic ranges for different waterbodies in the Southern Levant. **(A)** Enameloid phosphate oxygen isotope compositions ($\delta^{18}O_{PO4}$) of modern Mediterranean and Nile fish vs. the predicted $\delta^{18}O_{PO4}$ range expected for fish from these water bodies presented on a cross plot of $\delta^{18}O_{PO4}$ versus $\delta^{18}O_{Water}$ for seawater and Nile water, with isotherms of bioapatite formation calculated after Lécuyer et al. (2013). Note that modern Nile water is ^{18}O-enriched due to evaporation after building of the Aswan High Dam (Bialik and Sisma-Ventura, 2016) and thus has even slightly higher $\delta^{18}O_{Water}$ than the Mediterranean seawater. Therefore, calculated bioapatite $\delta^{18}O_{PO4}$ values for fish from Nile and Mediterranean seawater overlap. However, Sr isotopes are clearly distinct for both settings. The enameloid $\delta^{18}O_{PO4}$ values of fossil shark teeth from the City of David fall well into the expectation field for Late Cretaceous seawater based on Late Cretaceous shark teeth $\delta^{18}O_{PO4}$ values of Kolodny and Raab (1988) and Pucéat et al. (2003). **(B)** The $^{87}Sr/^{86}Sr$ from the Nile and Mediterranean represent two, clearly distinct endmembers of the water values encountered in the main fish-bearing water bodies in Egypt and the Southern Levant that are incorporated into fish teeth from the respective rivers, lakes and lagoons. Note that Lake Kinneret and Lake Manzala overlap in their $^{87}Sr/^{86}Sr$ as both have volcanically influenced fresh water sources. Late Cretaceous seawater values (range: 0.70729–0.70773; McArthur et al., 2020) also overlap with both waterbodies.

values taken from literature data and few measurements) and 38 observations from 14 modern fish specimens of known provenance (**Table 1** and **Supplementary Tables S4–S6**). In order to increase the sample size of data used to compute the LDF, specimens that underwent several Sr isotope analyses per tooth but only a single O isotope analysis were used. Thus a single $\delta^{18}O_{PO4}$ value was used for each $^{87}Sr/^{86}Sr$ measured in the same individual. Seven Bronze and Iron Age archaeological Gilthead seabream teeth were subsequently assigned a provenance to one of the six different water bodies using LDA. Provenance of the fossil, presumably Late Cretaceous sharks (n = 7; **Table 3**) was tested in a separate analysis (**Supplementary Table S7–S9**). For this purpose, Late Cretaceous seawater $^{87}Sr/^{86}Sr$ values taken from the LOWESS 6 Fit of McArthur et al. (2020) and $\delta^{18}O_{PO4}$ from Late Cretaceous shark teeth from Israel (Kolodny and Raab, 1988; Kolodny and Luz, 1991) were added to the reference dataset used to compute the LDF to assess the robusticity of the model (**Supplementary Tables S7–S9**). All values were transformed by subtracting the mean of the predictor's data from the observation's value and then by dividing by the standard deviation.

Accuracy of the groups assigned by the LDF were assessed with a confusion matrix using a "leave-one-out" cross-validation method, where an observation is omitted and then assigned by the LDF. The procedure is then repeated for each observation and allows for the success-rate of classification to be calculated (Friedman et al., 2001). All statistical analyses were performed using the statistical program R (version 4.0.2; R Core Team, 2018).

RESULTS

Shark Taxonomy and Biostratigraphic Age

All of the shark teeth displayed a grey-beige colouration and macroscopic preservation typical for Cretaceous fossil shark teeth from the Near East (**Supplementary Figure S1**). Several shark teeth were identified to the order of Lamniformes and some were assigned to *Squalicorax* sp. (Anacoracidae; n = 2), a taxon that only occurred during the Late Cretaceous (Shimada and Cicimurri, 2005, 2006). Another tooth was assigned to the family Odontaspididae (Sand shark; n = 1), also from the Cretaceous (**Figure 3B** and **Table 3**). The fossil nature of the shark teeth was further tested by analysing different mineralogical and geochemical proxies for diagenesis.

X-Ray Diffraction Analysis

The differences in crystallinity of the analysed fish tooth dentine samples are quite significant, and any peak broadening contribution from the instrument and sample preparation are considered to be negligible. The X-ray diffraction pattern of the dentine from four shark teeth exhibited three well-separated diffraction peaks (211, 112, 300) typical of recrystallised bioapatite in fossil dentine or bone (**Supplementary Figure S3**). In contrast, the dentine of the Chalcolithic Gilthead seabream teeth still had one broad diffraction peak, similar to the unaltered dentine of a modern Great white shark (**Supplementary Figure S3**). Therefore, the Gilthead seabream have a lower apatite crystallinity than the shark tooth samples. Fluorapatite was identified as the primary mineral phase, indicating diagenetic fluorine uptake into the dentine that would have originally consisted of a fluor-bearing hydroxylapatite in teleost fishes (<0.3 wt.% F; Suga et al., 1993). Modern shark dentine can contain high fluorine content (0.6–1.5 wt.%; Enax et al., 2012) in its carbonated bioapatite but this content is still much lower than in enameloid that consists of fluorapatite (3.1 wt.%; Enax et al., 2012; Kocsis et al., 2015). Some dentine samples (e.g., SK-84) also contained small amounts of calcite as a secondary diagenetic mineral infilling.

Total Organic Carbon (TOC) Analysis

The dentine of the four shark teeth had low TOC contents of 0.23 ± 0.26 wt.% (n = 4) which is more than 40 times lower than the TOC content of dentine in the modern Great white shark (9.54 wt.%) and more than eight times lower than in the dentine of Chalcolithic *Sparus aurata* teeth (1.99 ± 0.47 wt.%; n = 3) (**Supplementary Table S2** and **Supplementary Figure S4**).

Trace Element *in situ* LA-ICP-MS Analysis

Profiles of trace element content were measured across both dental tissues (enameloid and dentine) of all *S. aurata* (n = 5) and shark teeth (n = 7) from Chalcolithic and Iron Age cultural layers as well as one modern Great white shark and two *S. aurata* teeth as comparison to obtain unaltered dental tissue compositions (**Supplementary Figure S5** and **Supplementary Table S3**). Here we focus on two trace elements that are highly sensitive to diagenetic alteration – uranium and neodymium – to identify fossil specimens. Uranium and Nd are both typically only present in very low, ng/g-level concentrations in modern mammalian tooth bioapatite (Kohn et al., 1999) and also in modern fish teeth (Shaw and Wasserburg, 1985; Vennemann et al., 2001; Kocsis et al., 2015). The analysed modern Gilthead seabream and Great white shark dentine yield low Nd and U contents of 0.001–0.006 μg/g and 0.05–0.09 μg/g, respectively (**Figure 5**). This is in good agreement with the Nd content of 0.011 ± 0.011 μg/g in modern shark teeth (Shaw and Wasserburg, 1985; Vennemann et al., 2001). In contrast, the dentine of the shark teeth excavated from the City of David site had ≈ 100–1000 times higher U and Nd concentrations of ≈ 10–100 μg/g, typical for fossil dentine of shark teeth (Vennemann and Hegner, 1998; Kocsis et al., 2009). The dentine of the seabream teeth had intermediate Nd and U concentrations of ≈ 1–10 μg/g, and thus are ≈ 10–100 times enriched in U but less enriched in Nd as compared to the shark teeth (**Figure 5**). Enameloid is much less enriched (i.e., altered) in Nd and U compared to the dentine of the same tooth, both for Gilthead seabream and shark teeth.

Sr and O Isotope Data for Modern Fish Teeth and Bones

The $^{87}Sr/^{86}Sr$ and $\delta^{18}O_{PO4}$ data for modern sharks and bony fish from different water bodies in Egypt and the

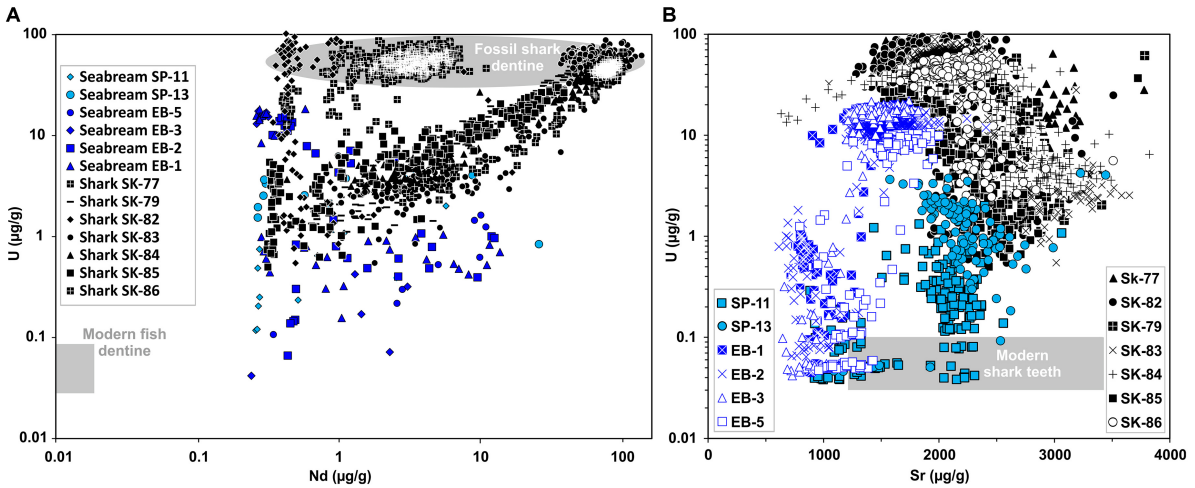

FIGURE 5 | Trace element compositions (U, Nd, Sr) of enameloid and dentine in ancient and modern Gilthead seabream and shark teeth measured by LA-ICP-MS line scans (**Supplementary Table S3**). Archaeological Gilthead seabream teeth are from the Chalcolithic and Iron Age periods and the Late Cretaceous fossil shark teeth are from the Iron Age cultural layers of the City of David, Jerusalem. **(A)** Cross plot of U and Nd concentrations. Note the logarithmic scale of both axes. Modern fish tooth dentine Nd and U field drawn after data from Vennemann et al. (2001) and this study. Fossil shark teeth have much higher dentine U and Nd contents than archaeological Gilthead seabream teeth. **(B)** Uranium (U) and strontium (Sr) concentration in fish teeth. Note the logarithmic scale of the *y*-axis. The grey Sr and U field for modern shark teeth is based on Sr concentrations from Vennemann et al. (2001) and Kocsis et al. (2015), U concentrations from this study. Note, despite U enrichment enameloid Sr concentrations of both archaeological Gilthead seabream and fossil shark teeth are still in the range of modern sharks.

Southern Levant are summarised in **Table 2** and are presented with respect to the expected values for each water body (**Figure 6**). A typical modern marine $^{87}Sr/^{86}Sr$ of ≈ 0.7092 was measured in tooth enameloid of extant deep-sea Gulper shark (*Centrophorus granulosus*) from the east Mediterranean, in European conger eels (Congridae; *Conger conger*), in native Eastern Mediterranean (Haifa Bay, Israel) Gilthead seabream (Sparidae; *Sparus aurata*) and also in Red Sea Sandbar shark (*Carcharinus plumbeus*). The high $\delta^{18}O_{PO4}$ values of both *C. granulosus* and *C. conger*, between 24.0 and 24.6‰ (**Table 2**), is a function of the low Mediterranean deep-water temperature range of 13–15°C and the deep-water $\delta^{18}O_{Water}$ value of 1.5 ± 0.2‰ (1 SD) (Sisma-Ventura et al., 2016). *S. aurata* $\delta^{18}O_{PO4}$ values of 22.5–23.5‰ (Sisma-Ventura et al., 2015, 2018) reflect the southeast Mediterranean coastal water temperature range of 17–30°C and the $\delta^{18}O_{Water}$ range between 1.4 and 1.9‰ (Sisma-Ventura et al., 2014, 2015). All extant Mediterranean fish fall within the range of seawater $^{87}Sr/^{86}Sr$ and $\delta^{18}O_{PO4}$ expected for marine fish (**Figure 6**) as well as the $^{87}Sr/^{86}Sr$ and the $\delta^{18}O_{PO4}$ values of the Red Sea Sandbar shark (**Table 2**).

Teeth of Blue fish (Pomatomidae; *Pomatomus salatrix*) from the Kishon River estuary yielded $^{87}Sr/^{86}Sr$ of 0.70901 ± 0.00006 (2 SE) and $\delta^{18}O_{PO4}$ value of 19.0 ± 0.3‰ (1 SD), which are lower than values for marine fish. Nevertheless, the Blue fish values agrees well with the expected $^{87}Sr/^{86}Sr$ and $\delta^{18}O_{PO4}$ values of the Kishon estuary, which is controlled by mixing of Israeli coastal groundwater and Mediterranean seawater (**Figure 6** and **Table 4**). The $^{87}Sr/^{86}Sr$ of extant freshwater fish from the Nile (Egypt) and Lake Kinneret (Israel), exhibited lower values between 0.707 and 0.708. The $^{87}Sr/^{86}Sr$ of extant Nilotic fish: Nile tilapia (Cichlidae; *Oreochromis niloticus*), upside-down catfish (Mochokidae: *Synodontis schall*) and bagrid catfish (Bagridae; *Bagrus bajad*) caught at different places in the Nile are very similar, yielding an average of 0.7071 ± 0.0002 (1 SD) and likewise for extant freshwater fish from Lake Kinneret (0.7073 ± 0.0003, 1 SD; **Figure 6** and **Table 4**). This similarity results from the fact that the drainage area of both freshwater bodies is comprised of extended volcanic bedrocks with low $^{87}Sr/^{86}Sr$ (Krom et al., 1999; Hartman and Richards, 2014).

Relatively high $\delta^{18}O_{PO4}$ values were observed in extant Nilotic fish, ranging between 20.1 and 24.5‰, reflecting the Nile's source water which derives from monsoonal rains ($\delta^{18}O_{Water}$ range of −3.0 to 0.0‰; Schilman et al., 2001) with additional ^{18}O-enrichment due to evaporation effects along the Nile trajectory through the desert and in the Aswan High Dam (Bialik and Sisma-Ventura, 2016).

Three species of extant freshwater cyprinids were analysed for their $^{87}Sr/^{86}Sr$: *Luciobarbus longiceps*, *Carasobarbus canis*, and *Capoeta damascina*. The first two species have $^{87}Sr/^{86}Sr$ that vary between 0.70731 and 0.70757, agreeing well with water from different depths of Lake Kinneret which have an average $^{87}Sr/^{86}Sr$ of 0.70750 ± 0.00005 (2 SE) (Fruchter et al., 2017). Even lower values, between 0.70681 ± 0.00008 and 0.70729 ± 0.00006 (2 SE) were obtained for the *C. damascina* samples. Modern Lake Kinneret fish display a large $\delta^{18}O_{PO4}$ range between 13.8 and 20.1‰, reflecting the local hydrological conditions with an average rainwater $\delta^{18}O_{Water}$ value around −7.0 to −6.0‰ (Gat and Dansgaard, 1972) and the strong evaporation effects in the Kinneret basin that lead to an ^{18}O-enrichment in the

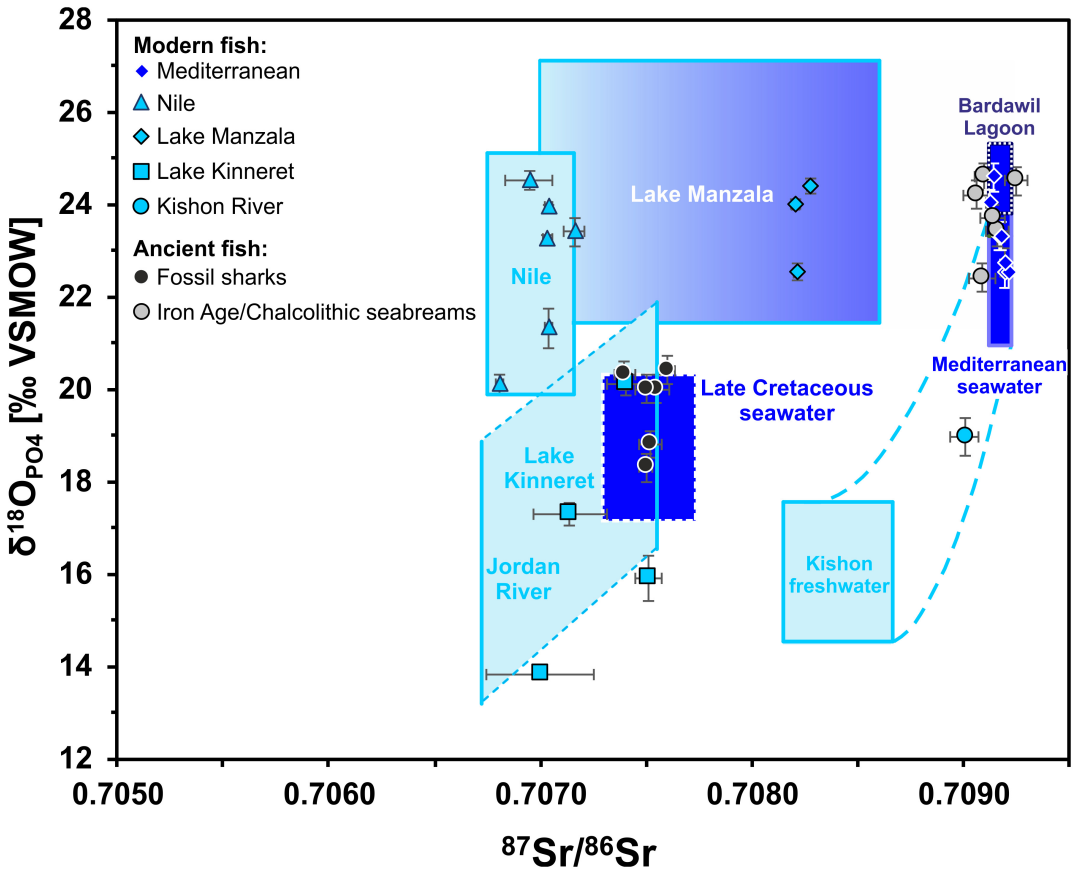

FIGURE 6 | Cross plot of $^{87}Sr/^{86}Sr$ versus $\delta^{18}O_{PO4}$ isotope data for modern fish teeth from Egypt and Israel as well as archaeological (Chalcolithic and Iron Age) Gilthead seabream and fossil shark teeth from the Southern Levant. Fish tooth $^{87}Sr/^{86}Sr$ and $\delta^{18}O_{PO4}$ data are plotted in comparison to the expected ranges of the fish habitats, calculated based on published water data (see text for details and **Table 4**). Note that all modern fish teeth fall within the according expected isotopic ranges of the water bodies in which they were captured. The modern blue fish from the brackish Kishon River estuary falls within the calculated range of mixed Mediterranean seawater and Israeli groundwater (blue stippled lines), with Kishon River as the primary freshwater source. Note the fossil marine sharks fall within the expectation field for Late Cretaceous seawater and do not overlap with any modern marine influenced water body.

lake water resulting in $\delta^{18}O_{Water}$ values between −2.5 and 0.0‰ (**Figure 6**; Gat, 1970).

Linear discriminant analysis was performed on water samples of known provenance and associated modern fish tooth samples for cross-validation, producing an error rate of 18%. This is due to the multiple partial overlaps in $^{87}Sr/^{86}Sr$ and $\delta^{18}O_{PO4}$ values from the different bodies of water: Bardawil Lagoon with the Mediterranean Sea, and the Nile River with both Lake Manzala as well as Lake Kinneret/Jordan River (**Figures 4, 6** and **Table 4**). Nevertheless, more than 80% of the modern fish of known provenance were correctly assigned to their respective water bodies using LDA (**Supplementary Table S4**).

Sr and O Isotope Data of Archaeological and Fossil Fish Teeth

The $^{87}Sr/^{86}Sr$ and $\delta^{18}O_{PO4}$ data of sharks and *S. aurata* from Chalcolithic and Iron Age archaeological layers of Israel are summarised in **Table 3** and shown in **Figure 6**. The shark teeth obtained from the Iron Age I-II periods of Jerusalem, all yielded unexpectedly low enameloid $^{87}Sr/^{86}Sr$ and $\delta^{18}O_{PO4}$ values for contemporaneous sharks, ranging between 0.7074 and 0.7076, and between 18.3 and 20.7‰, respectively. Placing the $^{87}Sr/^{86}Sr$ of the seven shark teeth on the Sr seawater curve (McArthur et al., 2020) yields Late Cretaceous Sr stratigraphic ages ranging from 86.5 to 76.3 Ma (**Table 3**) with an average late Santonian/early Campanian age of around 80.29 Ma +3.24, −2.64 Ma. The age uncertainties include analytical uncertainties, the 95% confidence interval of the Sr seawater curve, as well as the standard deviation of the calculated Sr stratigraphic ages. Six shark teeth cluster between 76.3 to 80.7 Ma (early Campanian). Only specimen SK-86 yields an older age of 86.5 Ma (latest Cenomanian/early Santonian) (**Table 3**). Their $\delta^{18}O_{PO4}$ are in good agreement with those of Campanian fossil fish teeth (teleosts and sharks) from Israel and Jordan ranging from 18.3 to 20.0‰ (Kolodny and Raab, 1988). In contrast, *S. aurata* teeth from similar archaeological contexts exhibited marine $^{87}Sr/^{86}Sr$ of around 0.7092, typical for modern seawater, and $\delta^{18}O_{PO4}$ values that agree well with the range expected for fish from

Mediterranean surface water or the hypersaline water of the Bardawil Lagoon (**Figures 4A, 6**), which formed as the result of seawater evaporation at the north Sinai coast.

To assign a provenance to archaeological fish samples, LDA was performed using the modern water and fish tooth reference dataset. All Chalcolithic/Iron Age seabream specimens were assigned to either the Bardawil Lagoon (50%, n = 3) or to the Mediterranean Sea (50%, n = 3) (**Supplementary Tables S4–S6**). Both Iron Age seabream teeth SP-11 and SP-13 from the City of David as well as one Chalcolithic specimen (EB-5) from Gilat (also with a high, Bardawil-like, $\delta^{18}O_{PO4}$ value) derive from the hypersaline Bardawil Lagoon. The other three seabream specimens from Gilat were all assigned a Mediterranean provenance (**Supplementary Table S5**). For the fossil shark teeth, all specimens were assigned to the Late Cretaceous seawater field, except for sample SK-83 (**Supplementary Tables S7–S9**). The LDA gave the same result when Late Cretaceous seawater values were restricted to those of the Campanian period. In both scenarios the sample SK-83 was assigned to Lake Kinneret/Jordan River, which is obviously incorrect for an 80 million-year-old fossil shark, and thus is best explained by the overlap of the two water bodies in Sr and O isotope space. Note also the incorrect assignment of the Nile perch (*Lates niloticus*) to the Mediterranean (**Supplementary Table S5**), resulting from diagenetic alteration of its bone Sr isotope composition (**Figure 7**).

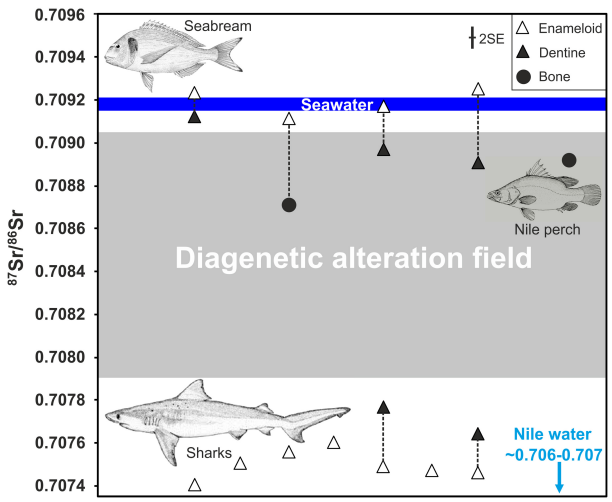

FIGURE 7 | Strontium isotope ratios of pairs of enameloid and dentine of fossil shark and archaeological Gilthead seabream (*Sparus aurata*) teeth from Iron Age (Jerusalem, City of David) and Chalcolithic (Gilat) archaeological sites (**Table 3**). A Nile perch vertebra bone from the Iron Age site of Ashkelon and one jawbone from *S. aurata* from the City of David are also plotted. Both are clearly diagenetically altered and fall within the range of values expected due to diagenetic alteration (grey field) defined by the range of $^{87}Sr/^{86}Sr$ for soil and rainwater compositions from Israel (**Table 4**). In contrast, none of the enameloid samples seem to be affected by diagenesis and instead preserve the original water $^{87}Sr/^{86}Sr$ of the Gilthead seabream and shark habitats. Note that all seven shark enameloid samples from different taxa have low $^{87}Sr/^{86}Sr$ between 0.7074 and 0.7076 reflecting Late Cretaceous (mostly Campanian) seawater values (McArthur et al., 2020).

DISCUSSION

Using fish tooth enameloid $^{87}Sr/^{86}Sr$ and $\delta^{18}O_{PO4}$ values collected from extant fish from different water bodies in Egypt and the Southern Levant enabled us to establish an isotopic reference dataset, which we then used as an interpretive framework for inferring the provenance of ancient *S. aurata* and different shark species recovered in coastal and inland archaeological layers from the Chalcolithic and Iron Age I-II periods (**Figure 2A**). *Post mortem* diagenetic alteration was carefully assessed to ensure that the original Sr and O isotope compositions are well preserved and still reflect the isotope values of the ambient water of the fish habitat. Fish taxonomic identification, combined with XRD, TOC and trace element (i.e., REE, U) analysis of dentine clearly demonstrated that the *S. aurata* teeth are sub-fossil archaeological fish teeth while the shark teeth from the same Iron Age cultural layers are all fossil teeth, most likely from the Late Cretaceous.

Variation of $^{87}Sr/^{86}Sr$ in Extant Shark and Bony Fish as Marker of Their Habitat

Marine shark and bony fish tooth enameloid both record the $^{87}Sr/^{86}Sr$ of ambient seawater. Hence, extant sharks from different oceanic basins and water depths with different hydrological conditions in temperature and salinity have rather uniform, seawater-like tooth $^{87}Sr/^{86}Sr$ values, averaging 0.709167 (range: 0.709160–0.709172, n = 8; Vennemann et al., 2001). In this study we obtained a similar value of 0.70919 ± 0.00005 (2 SE, n = 2; **Table 2**) for extant sharks from the Mediterranean (*Centrophorus granulosus*) and from the Red Sea (*Carcharinus plumbeus*), which matches the modern-day global seawater value of 0.70918 (McArthur et al., 2020). Similarly, tooth enameloid of modern *S. aurata* from the Eastern Mediterranean Sea also yields a typical marine values (**Table 2**). Much lower $^{87}Sr/^{86}Sr$, between 0.70681 ± 0.00008 and 0.70757 ± 0.00005 (2 SE), were measured in the teeth of three species of modern Cyprinidae from Lake Kinneret, which receives its water from the Golan Heights drainage area that is mainly underlain by basaltic bedrocks (Hartman and Richards, 2014). The two freshwater cyprinids *Luciobarbus longiceps* and *Carasobarbus canis* have $^{87}Sr/^{86}Sr$ that vary between 0.70731 and 0.70757, agreeing well with Lake Kinneret water with an average $^{87}Sr/^{86}Sr$ of 0.70750 ± 0.00005 (2 SE) (Fruchter et al., 2017). Even lower values, between 0.70681 ± 0.00008 and 0.70729 ± 0.00006 (2 SE), were obtained for the *C. damascina* samples that are in good agreement with the Sr isotope composition of the main fresh water source of Lake Kinneret and the Jordan River, which has an average $^{87}Sr/^{86}Sr$ of 0.70678 ± 0.00006 (1 SD) (Fruchter et al., 2017). This is well in line with the known migration behavior of some Cyprinidae species, including *C. damascina*, between Lake Kinneret and the Jordan River (Fishelson et al., 1996). All of these results further support the argument that fish, including sharks, record the $^{87}Sr/^{86}Sr$ of their ambient water. All extant marine and freshwater fish fall well within their respective expected isotopic ranges for the aquatic habitats in which they were caught (**Figure 6**). This

was supported by Linear Discriminant (LDA) analysis, which correctly assigned more than 80% of the modern fish to the correct water bodies based on their tooth Sr and O isotope composition (**Supplementary Table S4**).

Nilotic fish teeth and bones have $^{87}Sr/^{86}Sr$ between 0.70681 and 0.70737 (**Table 2** and **Figure 6**), which are in good agreement with modern Nile water values ranging from 0.70600 to 0.70718 (Brass, 1976; Gerstenberger et al., 1997; this study; **Table 4**). Similar values occur in freshwater fish from Lake Kinneret and the Jordan River. This similarity results from the fact that the drainage area for each of these water bodies is underlain by volcanic bedrocks. In this case, the coupling of $^{87}Sr/^{86}Sr$ and $\delta^{18}O_{PO4}$ data from the same teeth can be used to further differentiate fish from different aquatic habitats with similar bedrock types (and hence dissolved Sr of similar $^{87}Sr/^{86}Sr$) in their drainage area, but different hydrological regimes (i.e., water sources, salinities and/or degree of evaporation).

Assessing *Post Mortem* Diagenetic Alteration and Fish Provenance

Post mortem diagenetic alteration in the burial environment may have overprinted and shifted the original marine Sr isotope signature of fish teeth toward lower $^{87}Sr/^{86}Sr$. We assess diagenetic alteration by comparing the $^{87}Sr/^{86}Sr$ of dentine, which is much more prone to alteration than enamel (oid) (Ayliffe et al., 1994; Hoppe et al., 2003; Tütken et al., 2008), to that of enameloid from the same tooth (**Figure 7**). Both dental tissues record *in vivo* the same $^{87}Sr/^{86}Sr$ of the ambient water (**Table 2**; Vennemann et al., 2001; Tütken et al., 2011) but *post mortem* dentine is more prone to exchange of Sr with water in the soil (Tuross et al., 1989; Becker et al., 2008), similar to bone (Nelson et al., 1986; Hoppe et al., 2003). Thus, $^{87}Sr/^{86}Sr$ of dentine and bone are both expected to shift toward diagenetic soil water values more easily than enameloid. To infer Sr isotopic compositions of potential diagenetic fluids, rain and bedrock $^{87}Sr/^{86}Sr$ in Israel are considered (**Figure 7** and **Table 4**).

The main soil types in the area where the fish teeth were excavated are Rendzina, which typically has $^{87}Sr/^{86}Sr$ between 0.7079 and 0.7084 and Terra rossa, with a mean value of 0.70857 ± 0.00026 (1 SD) (Hartman and Richards, 2014). Both soils developed by weathering over Cretaceous-Eocene marine sedimentary rocks, thus soil pore water values are expected to have similar $^{87}Sr/^{86}Sr$ (**Table 4**). Several studies have demonstrated that Sr from pore water in soils can exchange with bioapatite (Nelson et al., 1986; Hoppe et al., 2003). Thus, diagenetic alteration would be expected to shift $^{87}Sr/^{86}Sr$ toward soil water values. Indeed, the dentine of the Chalcolithic *S. aurata* teeth shows slight modification toward the soil water field, as do the fossil shark teeth from Jerusalem.

Furthermore, the $^{87}Sr/^{86}Sr$ measured in modern rainwater samples from Israel range between 0.7079 and 0.7092 (mean 0.7087 ± 0.0004, 1 SD; n = 18; Herut et al., 1993; Frumkin and Stein, 2004). The major sources contributing to the $^{87}Sr/^{86}Sr$ in rainfall are Cretaceous-Eocene marine sedimentary rocks, dissolved Mid-Cretaceous-Eocene chalk dust from the Sahara (0.7078) and small quantities of sea spray (0.7092) (Herut et al., 1993). However, none of these Sr sources has low enough $^{87}Sr/^{86}Sr$ to explain the values we obtained from the fossil shark teeth from the Iron Age cultural layers. Groundwater from Late Cretaceous aquifers of Israel have low $^{87}Sr/^{86}Sr$ of around 0.7075 but these deep aquifers are located further inland in the Judean and Samarian arches (Starinsky et al., 1980) and thus cannot have contributed Sr to cause diagenetic alteration in the archaeological sites investigated.

Thus, the low enameloid $^{87}Sr/^{86}Sr$ of the shark teeth cannot be explained by diagenesis as no potential Sr source with such low values is present in the burial setting. In contrast, diagenesis should increase the $^{87}Sr/^{86}Sr$ of the shark teeth, as occurs in the dentine of the same teeth, which are clearly altered (**Figure 5**) and shifted to higher $^{87}Sr/^{86}Sr$ (**Figure 7**). Even if some degree of diagenesis is invoked, the original shark enameloid $^{87}Sr/^{86}Sr$ are even lower, suggesting that measured data should be considered as maximum values. Regardless, any significant alteration is rather unlikely as enameloid of marine *S. aurata* still reflects expected seawater $^{87}Sr/^{86}Sr$ within an uncertainty of 0.00002 (2 SE) and is not shifted toward lower values of the diagenetic soil water endmember, as is the case for the dentine/bone of the same teeth/fish (**Figure 7**). Therefore, their original enameloid $^{87}Sr/^{86}Sr$ is very likely preserved.

Moreover, the dentine in the shark teeth has higher $^{87}Sr/^{86}Sr$ than the enameloid, approaching $^{87}Sr/^{86}Sr$ of bedrocks and rainfall in the study area (**Figure 7**). In contrast, dentine $^{87}Sr/^{86}Sr$ of *S. aurata* are shifted to lower values compared to the seawater-like enameloid values. Thus, dentine $^{87}Sr/^{86}Sr$ of both sharks and *S. aurata* converge on the diagenetic fluid values, which are controlled by the local bedrock substrate (**Figure 7**). The opposing directions of the isotopic shifts in $^{87}Sr/^{86}Sr$ between the enameloid-dentine/jawbone pairs of shark and *S. aurata* teeth further support preservation of original enameloid $^{87}Sr/^{86}Sr$ in fish teeth. Therefore, we can conclude that original, low enameloid $^{87}Sr/^{86}Sr \approx 0.7075$ values in the shark teeth and high, modern seawater-like enameloid $^{87}Sr/^{86}Sr \approx 0.7092$ in *S. aurata* teeth from the same layers are still preserved. The shark enameloid $^{87}Sr/^{86}Sr$ fall well into the Late Cretaceous seawater field (**Figure 6**), as expected based on the taxonomic identification of some of the shark teeth (i.e., *Squalicorax* sp.) to Late Cretaceous taxa. Thus, these shark teeth are clearly fossils although they were found together with thousands of other archaeological fish remains in Iron Age cultural deposits (**Table 1**).

Sparus aurata is a marine fish with a unique life cycle that includes exploitation of hypersaline lagoons (Tancioni et al., 2003). We observed elevated $\delta^{18}O_{PO4}$ values in the teeth of *S. aurata*, implying that these fish originated from closed or semi-closed water bodies with a high degree of evaporation, such as the hypersaline Bardawil Lagoon situated on the Northern Sinai coast in Egypt (Kolodny et al., 1983; Sisma-Ventura et al., 2015, 2018, 2019). A high rate of evaporation increases the $\delta^{18}O_{Water}$ of the Mediterranean seawater from which the shallow, nearshore Bardawil Lagoon forms. It does not, however, change its water $^{87}Sr/^{86}Sr$. This was confirmed by strontium isotope

analysis of a water sample taken from the Bardawil Lagoon in January 2019 yielding a $^{87}Sr/^{86}Sr$ of 0.70916 ± 0.00002 (2 SE) which is the same (within error) as the value for hypersaline eastern Mediterranean seawater (0.709172; Reinhardt et al., 2001 and references therein; **Table 4**). One *S. aurata* tooth from Gilat (EB-5) and two from the City of David (SP-11, SP-13) are characterised by hypersaline $\delta^{18}O_{PO4}$ (**Figure 4A**) and seawater-like $^{87}Sr/^{86}Sr$ (**Figure 4** and **Table 3**). Based on their Sr and O isotope signature, the LDA assigned 50% (three out of six) of the archaeological *S. aurata* teeth to a hypersaline water origin, most likely the Bardawil Lagoon, and the remainder to the Mediterranean (**Supplementary Table S5**). This agrees well with previous $\delta^{18}O_{PO4}$ results for *S. aurata* teeth from other Late Bronze Age to Iron Age sites in Israel and indicates a Bardawil Lagoon origin for these fish (Sisma-Ventura et al., 2018). Thus, seabreams were presumably exported from Northern Egypt (Bardawil Lagoon) to the Southern Levant (specifically to the City of David, Jerusalem) during the Iron Age, and perhaps even as early as the Chalcolithic. Since there are no indications for hypersaline lagoons (only for some brackish lagoons) along the Israeli coast during the Holocene (Sivan et al., 2011, 2016), the Bardawil and/or other hypersaline lagoons must have existed elsewhere in the Southern Levant.

Finally, while the $^{87}Sr/^{86}Sr$ of the dentine of *S. aurata* is only somewhat altered by diagenesis, the $^{87}Sr/^{86}Sr$ (0.70892 ± 0.00006, 2 SE) of the Iron Age Nile perch vertebra from the coastal site of Ashkelon (**Figure 7**) is strongly altered and clearly shifted by >0.002 from expected Nilotic values ≈ 0.706 to 0.707 (Brass, 1976; Gerstenberger et al., 1997; **Table 4**) toward a much higher $^{87}Sr/^{86}Sr$ within in the soil water alteration field (**Figure 7**). This indicates that fish vertebrae, although abundant in archaeological sites, are prone to diagenetic alteration and thus not suitable to assess fish provenance.

Assessing the Origin and Age of Fossil Shark Teeth From Jerusalem

Some of the shark teeth recovered from strata dated to the 8–9th century BCE (Iron Age I-II) (Reich et al., 2007, 2008) in the City of David, Jerusalem, were identified (based on morphology) as extinct species from the Upper Cretaceous (e.g., *Squalicorax*). All shark teeth (including those which were not taxonomically identifiable), display trace element signatures of high U and Nd contents (**Figure 5A**), typical for fossilised fish teeth (Staudigel et al., 1985; Pucéat et al., 2003; Kocsis et al., 2009). This was further supported by the high apatite crystallinity (**Supplementary Figure S3**) and low organic carbon content of the dentine (**Supplementary Figure S4**) typical for fossil specimens but different from archaeological *S. aurata* teeth from the same cultural layers (thus, providing a special case for which the $^{87}Sr/^{86}Sr$ can be used as a tool to date marine fossils deposited in much younger archaeological contexts). This could improve our understanding regarding the extent and the meaning of this phenomenon in archaeological sites.

The $^{87}Sr/^{86}Sr$ values of these fossil shark teeth do not fit the modern reference dataset compiled for contemporaneous fish in the southern Levant. The mean enameloid $^{87}Sr/^{86}Sr$ value of 0.70751 ± 0.00006 (1 SD; n = 7) of the fossil shark teeth from Jerusalem is much lower than the $^{87}Sr/^{86}Sr$ measured in modern sharks (≈ 0.70917, **Table 2** and **Figure 6**), but agrees well with Late Cretaceous seawater $^{87}Sr/^{86}Sr$ values. These sharks likely incorporated Sr ($^{87}Sr/^{86}Sr$ ≈ 0.7075) from a Late Cretaceous marine habitat as they fall into the Late Cretaceous seawater field according to the LDA (**Supplementary Table S8**). Indeed, age estimates using the $^{87}Sr/^{86}Sr$ seawater curve of McArthur et al. (2020) place these teeth at late Santonian/early Campanian age of around 80.29 Ma +3.24, −2.64 Ma (range: 76.3–86.5 Ma; **Table 3**). This age was further supported by the $\delta^{18}O_{PO4}$ values of fossil shark teeth from Jerusalem, agreeing well with the range of $\delta^{18}O_{PO4}$ between 18.3 and 20.0‰ of late Santonian to late Campanian shark teeth from the Southern Levant, i.e., Negev Desert (Kolodny and Raab, 1988). Assuming a seawater $\delta^{18}O$ of −1‰ for a continental ice-free Earth, marine temperatures in the subtropical zone (i.e., 30–35° N) were estimated to around 28–29°C in the Cenomanian-Turonian period (Pucéat et al., 2003). The low shark enameloid $\delta^{18}O_{PO4}$ values thus reflect tooth formation in the warm shallow, tropical seawater of the Tethys Ocean shelf (Kolodny and Raab, 1988).

The recovery of a relatively large number of shark teeth in the Iron Age assemblage of the City of David together with diverse fish remains is puzzling for two main reasons: (1) shark teeth are rare in archaeological sites in the Southern Levant (**Table 1**); (2) this study clearly demonstrates that these shark teeth are fossils and hence do not represent shark consumption. Instead the presence of these teeth may reflect collection for other cultural purposes (tools, pendants, etc.), as has been observed in different contexts worldwide (Cione and Bonomo, 2003; Betts et al., 2012; Charpentier et al., 2020). Alternatively, the fossils were simply a component of the local soil substrate and derive from weathering processes of the Late Cretaceous limestone substrate. However, this is not very likely as the Late Cretaceous marine sedimentary strata beneath the City of David are stratigraphically older (Turonian; **Figure 8**) than the Sr-stratigraphic age of the fossil shark teeth (late Santonian/early Campanian). However, fossil shark teeth from the Late Cretaceous are abundant in the marine sediments of the Mount Scopus group in Israel and in the Menuha Formation of the Southern Negev (**Figure 2A**; Gvirtzman, 2004; Gvirtzman et al., 2008; Wilson et al., 2012; Retzler et al., 2013).

Shark teeth recovered in the City of David were mainly from the "Rock Cut Pool" (**Figure 2B**; note that the complete area of this structure was fully excavated and sieved, Reich et al., 2007, 2008), and from area G, a mixed dump deposition, dated to *ca.* 586 BCE (Lernau, 2015). In area G, nine shark teeth were recovered, but these were not used in this study. However, except for these two locations, no fossil shark teeth have been reported from geological strata in the city of David or anywhere else in Jerusalem. Thus, the fossil shark teeth found in the City of David are probably not derived from the underlying marine limestone and dolomite of the Shivta Formation, which is of Turonian age (Rosenfeld and Hirsch, 2005; **Figure 8**), and is thus older than the Santonian/Campanian age inferred by Sr stratigraphy for the

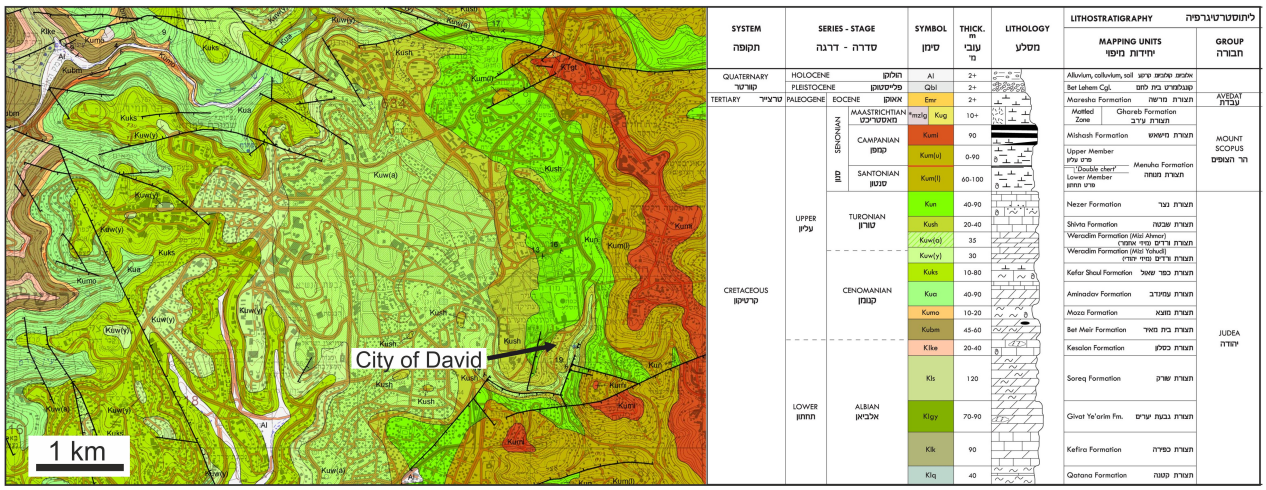

FIGURE 8 | Geological map of Jerusalem with the City of David modified from Rosensaft and Sneh (2011). Therefore, rock formation names are provided in both English and Hebrew (as provided in the official geological map of Jerusalem). The City of David is situated on marine sedimentary strata of the Shivta Formation being Turonian in age. Note that the fossil shark teeth found in the Iron Age strata yielded younger late Santonian/early Campanian Sr stratigraphic ages. Such fossil shark teeth are only known from the Menuha Formation of the Mount Scopus group in the Negev Desert (Kolodny and Raab, 1988; Retzler et al., 2013). These shark teeth bearing outcrops are 90 km up to 180 km south of Jerusalem in the Negev Desert (**Figure 2A**). Note that sediments of the Menuha Formation also crop out at the hillslopes a few hundred meters east/southeast of the City of David, however, no fossil shark teeth were reported from these strata.

fossil shark teeth. However, Turonian (0.70732 ± 0.00002 1 SD) and Campanian (0.70758 ± 0.00008 1 SD) seawater $^{87}Sr/^{86}Sr$ differ on average by only 0.00026 (McArthur et al., 2020). Therefore, only a slight diagenetic alteration of the enameloid $^{87}Sr/^{86}Sr$ by +0.00016 would be sufficient to shift the value of Turonian shark teeth to the observed value 0.70751 and hence a late Santonian/early Campanian age. The dentine of two of the shark teeth was diagentically shifted by 0.0001–0.0002, yielding higher $^{87}Sr/^{86}Sr$ values compared to enameloid. Strontium isotopes in sub-mm sized Cenozoic fossil fish teeth from marine sediment drill cores are prone to diagenetic alteration (Martin and Scher, 2004). However, the fluorapatite of the enameloid of larger cm-sized shark teeth is less prone to diagenesis and still has low U and Nd contents (about 10 times lower compared to the dentine; **Figure 5A**) and no correlation was observed between Sr and U contents (**Figure 5B**), which could be taken as an indication against significant diagenetic alteration of the Sr isotope composition. The Sr stratigraphic age of the fossil shark teeth from the City of David fits perfectly to the Santonian to early Campanian age of the fossil shark teeth-bearing Menuha Formation in the southern Negev (Retzler et al., 2013). Therefore, we can conclude that these fossil shark teeth may have been collected in the Negev Desert up to 90 km south of Jerusalem (**Figure 2A**). For instance from the Letaot Mountain fossil shark teeth of late Santonian/early Campanian age are known (Kolodny and Raab, 1988). The Menuha Formation also crops out in hill slopes a few hundred meters to the east/southeast of the City of David (**Figure 8**), however, no finds of fossil shark teeth are reported from this or other areas in Jerusalem thus far. Therefore, it is entirely feasible that the fossil teeth were transported to the City of David although the reason for bringing these teeth to the city and their function remains elusive.

CONCLUSION

We establish a Sr and O isotope reference dataset for bioapatite of modern marine and freshwater fish from the Mediterranean, Bardawil Lagoon, Lake Kinneret, Jordan River and Nile River. Fish from these different water bodies in Egypt and the Southern Levant have distinct Sr and O isotope signatures that enable us to distinguish their provenance from Nilotic, hypersaline, marine and fresh water bodies using LDA. This will be an important asset for future provenance studies of archaeological fish remains in the Levant and will shed new light on the Levantine fish provenance and trade. Unexpectedly, multiple Late Cretaceous (80.3 ± 3.2 Ma) fossil shark teeth were encountered in the same Iron Age cultural layers of the City of David, Jerusalem together with a wide diversity of archaeological fish originating from the Mediterranean Sea and the Nile. These fossil shark teeth clearly do not represent food remnants although their use remains elusive. It may be they were brought to the city intentionally as the nearest fossil shark teeth bearing outcrops of Campanian age are situated in the Negev Desert (≈ 90 km south of Jerusalem), although similar aged strata also crop out near the City of David. Thus, in archaeological fish assemblages, fossil fish teeth can also be encountered. This should be carefully evaluated, and we here provide a toolset comprised of combined dentine XRD, TOC and trace element (i.e., U, REE) analysis to distinguish fossil from archaeological teeth based on degree of diagenetic alteration. In contrast, the enameloid of the fossil shark and the archaeological Gilthead seabream (*S. aurata*) teeth still preserves its original $^{87}Sr/^{86}Sr$ and $\delta^{18}O_{PO4}$ values. The Sr and O isotope signatures indicate that some of the Gilthead seabreams were not caught locally in the Mediterranean, but instead in the hypersaline water of the Bardawil Lagoon and were

imported from Egypt to coastal and inland sites in Israel during the Iron Age and probably already since the Chalcolithic. We demonstrate that this dual-isotope approach, frequently used to assess provenance of terrestrial vertebrates, is also a powerful toolset for tracing the provenance of fish and provides new insights into past human fish exploitation (even of fossil fish teeth) and trade patterns.

DATA AVAILABILITY STATEMENT

The original contributions presented in the study are included in the article/**Supplementary Material**, further inquiries can be directed to the corresponding author/s.

ETHICS STATEMENT

Ethical review and approval was not required for the animal study because we analysed modern staple food fish obtained from fishermen as well as archaeological and fossil fish teeth.

AUTHOR CONTRIBUTIONS

TT and GS-V designed the research. TT, GS-V, IZ, and MW wrote the manuscript. GS-V and TT interpreted the isotope data. HH, IZ, and OL provided and prepared the fish samples. IZ determined the fish species and provided the all fish related information. MW performed the Sr isotope and LA-ICP-MS analysis and evaluated the Sr isotope data. TT evaluated TOC, XRD and trace element data. NB performed the statistics using Linear Discriminant Analysis (LDA). GS-V prepared the tooth samples for oxygen isotope analysis. KJ provided the analytical facilities for Sr isotope analysis. All authors contributed to the article and approved the submitted version.

FUNDING

This project received funding from the European Research Council (ERC) under the European Union's Horizon 2020 Research and Innovation Programme (grant agreement no. 681450). MW is thankful to the Max Planck Graduate Center for funding.

ACKNOWLEDGMENTS

We thank Torsten Vennemann and Michael Maus for performing phosphate oxygen isotope measurements and Hubert Vonhof for running water samples for oxygen isotope analyses and the dentine for carbonate content. We thank B. Stoll and U. Weis for assistance in the LA-MC-ICP-MS laboratory. Modern Mediterranean fish were collected as part of the Israel Oceanographic and Limnological Research deep-sea national monitoring program. We thank Sabine Fiedler and Björn Glasner for total carbon analysis, Sven Brömme for TIC analysis, and Ralf Meffert for the XRD analysis of the dentine samples. Special thanks to Jürgen Kriwet for taxonomic shark tooth identification. Or Bilak is kindly acknowledged for discussing Cretaceous geology of Israel and fossil shark tooth occurrence. Menachem Goren, from the Steinhardt Museum, Tel Aviv University, provided us information regarding the biogeographic distribution of *Oreochromis niloticus*. We also thank especially Jennifer Leichliter for meticulously proofreading the English. Finally, yet importantly, we want to thank the two reviewers who helped with their constructive comments to significantly improve the manuscript. Especially the reviewer who pointed us to the possibility that the shark teeth from the archaeological layers could be fossil teeth, which was a game changer. It led us to perform additional analysis and, ultimately, to rework the narrative of the manuscript, changing the story from shark exportation from the Nile delta to fossil shark finds in cultural layers. This was a textbook example how a good review should work and we are very appreciative.

SUPPLEMENTARY MATERIAL

The Supplementary Material for this article can be found online at: https://www.frontiersin.org/articles/10.3389/fevo.2020.570032/full#supplementary-material

REFERENCES

Aly, A. I. M., Hamed, M. A., Abd El-Samie, S. G., and Eweida, E. A. (2004). Environmental isotopes and hydrochemistry approach to evaluate the source of recharge and pollution load in Manzala and Bardawil Lakes, Egypt (IAEA-CN-118/85). Isotopes in Environmental Studies Aquatic Forum Conference and Symposium Papers 26, 172–173.

Ayliffe, L. K., Chivas, A. R., and Leakey, M. G. (1994). The retention of primary oxygen isotope compositions of fossil elephant skeletal phosphate. *Geochim. Cosmochim. Acta* 58, 5291–5298. doi: 10.1016/0016-7037(94)90312-3

Bartosiewicz, L., Lisk, E., and Zohar, I. (2018). "Non-mammalian vertebrate remains," in *Excavations at Dor, Final Report. Volume IIB, Area G, The Late Bronze and Iron Ages: Pottery, Artifacts, Ecofacts and other studies, Qedem Reports*, eds A. Gilboa, I. Sharon, J. R. Zorn, S. Matskevich (Jerusalem: The Hebrew University of Jerusalem), 313–322.

Becker, M. A., Seidemann, D. E., Chamberlain, J. A., Buhl, D., and Slattery, W. (2008), Strontium isotopic signatures in the enameloid and dentine of upper Cretaceous shark teeth from western Alabama: paleoecologic and geochronologic implications. *Palaeogeogr. Palaeoclimatol. Palaeoecol.* 264, 188–194. doi: 10.1016/j.palaeo.2008.04.006

Berglund, M., and Wieser, M. E. (2011). Isotopic compositions of the elements 2009 (IUPAC Technical Report). *Pure Appl. Chem.* 83, 397–410. doi: 10.1351/pac-rep-10-06-02

Betts, M., Blair, S., and Black, D. (2012). Perspectivism, mortuary symbolism, and human-shark relationships on the Maritime Peninsula. *Am. Antiq.* 77, 621–645. doi: 10.7183/0002-7316.77.4.621

Bialik, O. M., and Sisma-Ventura, G. (2016). Proxy-based reconstruction of surface water acidification and carbonate saturation of the Levant Sea during the Anthropocene. *Anthropocene* 16, 42–53. doi: 10.1016/j.ancene.2016.08.001

Borhegyi, S. F. (1961). Shark teeth, stingray spines, and shark fishing in ancient Mexico and Central America. *Southwest. J. Anthropol.* 17, 273–296. doi: 10.1086/soutjanth.17.3.3629046

Botella, H., and Valenzuela-Ríos, J. I., and Martínez-Perez, C. (2009). Tooth replacement rates in early chondrichthyans: a qualitative approach. *Lethaia* 42, 365–376. doi: 10.1111/j.1502-3931.2009.00152.x

Boulanger, C., Puaud, S., Ly, V., Glémarec, L., Heng, S., and Forestier, H. (2020). Fishbone artefacts from the Samrong Sen site, Cambodia, cast new light on Bronze Age networking between inland and coastal communities. *Int. J. Osteoarchaeol.* doi: 10.1002/oa.2922

Brass, G. W. (1976). The variation of the marine $^{87}Sr/^{86}Sr$ ratio during Phanerozoic time: interpretation using a flux model. *Geochim. Cosmochim. Acta* 40, 721–730. doi: 10.1016/0016-7037(76)90025-9

Bryant, J. D., Jones, D. S., and Mueller, P. A. (1995). Influence of freshwater flux on 87Sr/86Sr chronostratigraphy in marginal marine environments and dating of vertebrate and invertebrate faunas. *J. Paleontol.* 69, 1–6. doi: 10.1017/s002233600002686x

Cappetta, H. (2012). "Mesozoic and Cenozoic Elasmobranchii: teeth. Chondrichthyes," in *Handbook of Palaeoichthyology, 3E*, ed. H. P. Schulze (München: Dr. Friedrich Pfeil), 512.

Chadwick, O. A., Derry, L. A., Vitousek, P. M., Huebert, B. J., and Hedin, L. (1999). Changing sources of nutrients during four million years of ecosystem development. *Nature* 397, 491–497. doi: 10.1038/17276

Charpentier, V., Adnet, S., and Cappetta, H. (2020). The tooth of a giant sea creature *Otodus* (*Megaselachus*) in the material culture of Neolithic maritime hunter-gatherers at Sharbithat (Sultanate of Oman). *Int. J. Osteoarchaeol.* doi: 10.1002/oa.2914

Chenery, C., Müldner, G., Evans, J., Eckardt, H., and Lewis, M. (2010). Strontium and stable isotope evidence for diet and mobility in Roman Gloucester, UK. *J. Archaeol. Sci.* 37, 150–163. doi: 10.1016/j.jas.2009.09.025

Cione, A., and Bonomo, M. (2003). Great white shark teeth used as pendants and possible tools by Early-Middle Holocene terrestrial mammal hunter-gatherers in the Eastern Pampas (Southern South America). *Int. J. Osteoarchaeol.* 13, 222–231. doi: 10.1002/oa.678

Davis, S. J. M. (1985). "A preliminary report of fauna from Hatula: a Natufian-Khiamian (PPNA) site near Latroun, Israel," in *Le site Natufian-Khiamien de Hatoula, pres de Latroun, Israel*, eds M. Lechevallier and A. Ronen (Jerusalem: Centre de Recherche Français de Jérusalem), 71–118.

De Groot, A., and Fadida, A. (2011). The Pottery Assemblage from the Rock Cut Pool near the Gihon Spring. *Tel Aviv* 38, 158–166. doi: 10.1179/033443511x13099584885501

Debiais-Thibaud, M., Borday-Birraux, V., Germon, I., Bourrat, F., Metcalfe, C., Casane, D., et al. (2007). Development of oral and pharyngeal teeth in the Medaka (*Oryzias latipes*): comparison of morphology and expression of eve1 Gene. *J. Exp. Zool. B Mol. Dev. Evol.* 308, 693–708. doi: 10.1002/jez.b.21183

Debiais-Thibaud, M., Chiori, R., Enault, S., Oulion, S., Germon, I., Martinand-Mari, C., et al. (2015). Tooth and scale morphogenesis in shark: an alternative process to the mammalian enamel knot system. *BMC Evol. Biol.* 15:292. doi: 10.1186/s12862-015-0557-0

Dettmann, I., Kohn, M., Quade, J., Reyerson, F. J., Ojah, T. P., and Hamidullah, S. (2001). Seasonal stable isotope evidence for a strong Asian monsoon throughout the past 10.7 Ma. *Geology* 29, 31–34. doi: 10.1130/0091-7613(2001)029<0031:ssiefa>2.0.co;2

Dufour, E., Holmden, C., Van Neer, W., Zazzo, A., Patterson, W. P., Degryse, P., et al. (2007). Oxygen and strontium isotopes as provenance indicators of fish at archaeological sites: the case study of Sagalassos, SW Turkey. *J. Archaeol. Sci.* 34, 1226–1239. doi: 10.1016/j.jas.2006.10.014

Enault, S., Guinot, G., Koot, M., and Cuny, G. (2015). Chondrichthyan tooth enameloid: past, present, and future. *Zool. J. Linn. Soc.* 174, 549–570. doi: 10.1111/zoj.12244

Enax, J., Janus, A. M., Raabe, D., Epple, M., and Fabritius, H.-O. (2014). Ultrastructural organization and micromechanical properties of shark tooth enameloid. *Acta Biomater.* 10, 3959–3968. doi: 10.1016/j.actbio.2014.04.028

Enax, J., Prymak, O., Raabe, D., and Epple, M. (2012). Structure, composition and mechanical properties of shark teeth. *J. Struct. Biol.* 118, 290–299. doi: 10.1016/j.jsb.2012.03.012

Fetner, R. A., and Iwaszczuk, U. (2020). Isotopic evidence of possible long-distance freshwater fish trade in the 13th to 14th century Chełm, modern Poland. *Int. J. Osteoarchaeol.* doi: 10.1002/oa.2931

Fischer, J., Schneider, J., Voigt, S., Joachimski, M., Tichomirowa, M., Tütken, T., et al. (2013). Oxygen and strontium isotopes from fossil shark teeth: environmental and ecological implications for Late Palaeozoic European basins. *Chem. Geol.* 342, 44–62. doi: 10.1016/j.chemgeo.2013.01.022

Fishelson, L., Goren, M., Van Vuren, J., and Manelis, R. (1996). Some aspects of the reproductive biology of *Barbus* spp., *Capoeta damascina* and their hybrids (Cyprinidae, Teleostei) in Israel. *Hydrobiologia* 317, 79–88. doi: 10.1007/bf00013728

Fradkin, A., and Lernau, O. (2006). "The fish bone remains," in *Tel Tanninim: Excavations at Krokodeilon Polis, 1996-1999*, ed. R. R. Stieglitz (Boston, MA: The American Schools of Oriental Research), 211–222.

Fradkin, A., and Lernau, O. (2008). "The fishing economy at Caesarea," in *Caesarea Reports and Studies: Excavations 1995-2007 within the Old City and the Ancient Harbor, BAR International Series 1784*, eds K. G. Holum, J. A. Stabler, and E. G. Reinhardt (Oxford: Archaeopress), 189–200.

Friedman, J., Hastie, T., and Tibshirani, R. (2001). *The Elements of Statistical Learning* (Vol. 1). (New York, NY: Springer).

Fruchter, N., Lazar, B., Nishri, A., Almogi-Labin, A., Eisenhauer, A., Be'eri Shlevin, Y., and Stein, M. (2017). $^{88}Sr/^{86}Sr$ fractionation and calcite accumulation rate in the Sea of Galilee. *Geochim. Cosmochim. Acta* 215, 17–32. doi: 10.1016/j.gca.2017.07.026

Frumkin, A., and Stein, M. (2004). The Sahara–East Mediterranean dust and climate connection revealed by strontium and uranium isotopes in a Jerusalem speleothem. *Earth Planet. Sci. Lett.* 217, 451–464. doi: 10.1016/s0012-821x(03)00589-2

Galili, E., Lernau, O., and Zohar, I. (2004). Fishing and coastal adaptations at 'Atlit-Yam- A submerged PPNC fishing village off the Carmel Coast, Israel. *Atiqot* 48, 1–34.

Garfinkel, Y., Dag, D., Hesse, B., Wapnish, P., Rookis, D., Hartman, G., Bar-Yosef Mayer, D. E., and Lernau, O. (2005). Neolithic Ashkelon: meat processing and early pastoralism on the Mediterranean coast. *Eurasian Prehist.* 3, 43–72.

Gat, J. R., and Dansgaard, W. (1972). Stable isotope survey of the fresh water occurrences in Israel and the northern Jordan rift valley. *J. Hydrol.* 16, 177–212. doi: 10.1016/0022-1694(72)90052-2

Gat, J. R. (1970). "Environmental isotope balance of Lake Tiberias," in *Proceedings of IAEA Symposium on Isotope Hydrology*, Vienna 109–127.

Gerstenberger, H., Haase, G., and Abou El Nour, F. (1997). The origin of strontium and the strontium isotope budget of the River Nile. *Isotopes Environ. Health Stud.* 33, 349–356. doi: 10.1080/10256019708234047

Goldstein, S. J., and Jacobsen, S. B. (1987). The Nd and Sr isotopic systematics of river-water dissolved material: implications for the sources of Nd and Sr in seawater. *Chem. Geol.* 66, 245–272. doi: 10.1016/0168-9622(87)90045-5

Gvirtzman, Z. (2004). Chronostratigraphic table and subsidence curves of southern Israel. *Isr. J. Earth Sci.* 53, 48–61. doi: 10.1560/krh0-1q21-u1yg-yh4h

Gvirtzman, Z., Zilberman, E., and Folkman, Y. (2008). Reactivation of the Levant passive margin during the late Tertiary and formation of the Jaffa Basin offshore central Israel. *J. Geol. Soc.* 165, 563–578. doi: 10.1144/0016-76492006-200

Harrell, T. L., Pérez-Huerta, A., and Phillips, G. (2016). Strontium isotope age-dating of fossil shark tooth enameloid from the Upper Cretaceous Strata of Alabama and Mississippi, USA. *Cretac. Res.* 62, 1–12. doi: 10.1016/j.cretres.2016.01.011

Hartman, G., and Richards, M. (2014). Mapping and defining sources of variability in bioavailable strontium isotope ratios in the Eastern Mediterranean. *Geochim. Cosmochim. Acta* 126, 250–264. doi: 10.1016/j.gca.2013.11.015

Herut, B., Starinsky, A., and Katz, A. (1993). Strontium in rainwater from Israel – sources, isotopes and chemistry. *Earth Planet. Sci. Lett.* 120, 77–84. doi: 10.1016/0012-821x(93)90024-4

Hobbs, J. A., Lewis, L. S., Willmes, M., Denney, C., and Bush, E. (2019). Complex life histories discovered in a critically endangered fish. *Sci. Rep.* 9:16772.

Hodell, D. A., Mead, G. A., and Mueller, P. A. (1990). Variation in the strontium isotope composition of seawater (8 Ma to present): implications for chemical weathering rates and dissolved fluxes to the oceans. *Chem. Geol.* 80, 291–307. doi: 10.1016/0168-9622(90)90011-z

Hoppe, K. A., Koch, P. L., and Furutani, T. T. (2003). Assessing the preservation of biogenic strontium in fossil bones and tooth enamel. *Int. J. Osteoarchaeol.* 13, 20–28. doi: 10.1002/oa.663

Horwitz, L. K., Bar Giora, N., Mienis, H. K., and Lernau, O. (2005). "Faunal and malacological remains from the Middle Bronze, Late Bronze, and Iron Age levels at Tel Yoqne'am," in *Yone'am II: The Middle and Late Bronze Ages. Final Report of the Archaeological Excavations (1977-1988), Qedem Reports*, eds A. Ben-Tor, D. Ben-Ami, and A. Livneh (Jerusalem: Qedem), 395–431.

Horwitz, L.K., and Lernau, O. (2018). "Iron Age IIb faunal remains from the Ophel, Area A2009," in *The Ophel Excavations to the South of the Temple Mount 2009-2013*, ed. E. Mazar (Shoam: Shoam Academic Research Publication), 289–309.

Ingle, C. P., Sharp, B. L., Horstwood, M. S. A., Parrish, R. R., and Lewis, D. J. (2003). Instrument response functions, mass bias and matrix effects in isotope ratio measurements and semi-quantitative analysis by single and multi-collector ICP-MS. *J. Anal. At. Spectrom.* 18, 219–229. doi: 10.1039/b211527a

Ingram, B. L. (1995). High-resolution dating of deep-sea clays using Sr isotopes in fossil fish teeth. *Earth Planet. Sci. Lett.* 134, 545–555. doi: 10.1016/0012-821x(95)00151-2

Irrgeher, J., Galler, P., and Prohaska, T. (2016). $^{87}Sr/^{86}Sr$ isotope ratio measurements by laser ablation multicollector inductively coupled plasma mass spectrometry: reconsidering matrix interferences in bioapatites and biogenic carbonates. *Spectrochim. Acta Part B At. Spectrosc.* 125, 31–42. doi: 10.1016/j.sab.2016.09.008

Jambura, P. L., Pfaff, C., Underwood, C. J., Ward, D. J., and Kriwet, J. (2018). Tooth mineralization and histology patterns in extinct and extant snaggletooth sharks, *Hemipristis* (Carcharhiniformes, Hemigaleidae)—Evolutionary significance or ecological adaptation? *PloS ONE* 13:e0200951. doi: 10.1371/journal.pone.0200951

Jambura, P. L., Türtscher, J., Kindlimann, R., Metscher, B., Pfaff, C., Stumpf, S., et al. (2020). Evolutionary trajectories of tooth histology patterns in modern sharks (Chondrichthyes, Elasmobranchii). *J. Anat.* 236, 753–771. doi: 10.1111/joa.13145

Jernvall, J., and Thesleff, I. (2012). Tooth shape formation and tooth renewal: evolving with the same signals. *Development* 139, 3487–3497. doi: 10.1242/dev.085084

Jochum, K. P., Pfänder, J., Woodhead, J. D., Willbold, M., Stoll, B., Herwig, K., et al. (2005). MPI-DING glasses: New geological reference materials for in situ Pb isotope analysis. *Geochem. Geophys. Geosys.* 6:Q10008. doi: 10.1029/2005GC000995

Klug, S., Tütken, T., Wings, O., Pfretzschner, H., and Martin, T. (2010). A Late Jurassic freshwater shark assemblage (Chondrichthyes, Hybodontiformes) from the southern Junggar Basin, Xinjiang, Northwest China. *Palaeobiodiv. Palaeoenviron.* 90, 241–257. doi: 10.1007/s12549-010-0032-2

Kocsis, L., Gheerbrant, E., Mouflih, M., Cappetta, H., Yans, J., and Amaghzaz, M. (2014). Comprehensive stable isotope investigation of marine biogenic apatite from the late Cretaceous-early Eocene phosphate series of Morocco. *Palaeogeogr. Palaeoclimatol. Palaeoecol.* 394, 74–88. doi: 10.1016/j.palaeo.2013.11.002

Kocsis, L., Vennemann, T. W., and Fontignie, D. (2007). Migration of sharks into freshwater systems during the Miocene and implications for Alpine paleoelevation. *Geology* 35, 451–454. doi: 10.1130/g23404a.1

Kocsis, L., Vennemann, T. W., Hegner, E., Fontignie, D., and Tütken, T. (2009). Constraints on the paleoceanography and paleoclimate of the Miocene north Alpine Molasse, Vienna and Pannonian Basins: records of the O-, Sr-, and Nd-isotope composition of marine fish and mammal remains. *Palaeogeogr. Palaeoclimatol. Palaeoecol.* 271, 117–129. doi: 10.1016/j.palaeo.2008.10.003

Kocsis, L., Vennemann, T. W., Ulianov, A., and Brunnschweiler, J. M. (2015). Characterizing the bull shark *Carcharhinus leucas* habitat in Fiji by the chemical and isotopic compositions of their teeth. *Environ. Biol. Fish.* 98, 1609–1622. doi: 10.1007/s10641-015-0386-4

Kohn, M. J., Schoeninger, M. J., and Barker, W. B. (1999). Altered states: effects of diagenesis on fossil tooth chemistry. *Geochim. Cosmochim. Acta* 63, 2737–2747. doi: 10.1016/s0016-7037(99)00208-2

Kolodny, Y., and Luz, B. (1991). *Oxygen Isotopes in Phosphates of Fossil Fish-Devonian to Recent. Stable Isotope Geochemistry: A Tribute to Samuel Epstein. The Geochemical Society, Special Publication No. 3.* (Washington, DC: Geochemical Society), 105–119.

Kolodny, Y., Luz, B., and Navon, O. (1983). Oxygen isotope variations in phosphate of biogenic apatites, I. Fish bone apatite – rechecking the rules of the game. *Earth Planet. Sci. Lett.* 64, 398–404. doi: 10.1016/0012-821x(83)90100-0

Kolodny, Y., and Raab, M. (1988). Oxygen isotopes in phosphatic fish remains from Israel: paleothermometry of tropical Cretaceous and Tertiary shelf waters. *Palaeogeogr. Palaeoclimatol. Palaeoecol.* 64, 59–67. doi: 10.1016/0031-0182(88)90142-3

Krom, M. D., Michard, A., Cliff, R. A., and Strohle, K. (1999). Sources of sediment to the Ionian Sea and western Levantine basin of the Eastern Mediterranean during S-1 sapropel times. *Mar. Geol.* 160, 45–61. doi: 10.1016/s0025-3227(99)00015-8

Lécuyer, C., Amiot, R., Touzeau, A., and Trotter, J. (2013). Calibration of the phosphate $\delta^{18}O$ thermometer with carbonate–water oxygen isotope fractionation equations. *Chem. Geol.* 347, 217–226. doi: 10.1016/j.chemgeo.2013.03.008

Lernau, O. (2004). Fish remains from Early Bronze Age Ashqelon, Afridar. *Atiqot* 45, 299–303.

Lernau, H. (1988). "Fish remains from two smelting camps and the Timna temple," in *The Egyptian Mining temple at Timna. Institute for Archaeo-Metallurgical Studies [and] Institute of Archaeology*, ed. B. Rothenberg (London: University College London), 241–246.

Lernau, H., and Lernau, O. (1994). "The Fish Remains," in *Le Gisement de Hatoula en Judee occidentale, Israel. Association Paléorient*, eds M. Lechevallier and A. Ronen (Paris: Mémoires et Travaux du Centre de Recherche Français de Jerusalem), 111–121.

Lernau, O. (1995). "The fish remains of Upper Zohar," in *Upper Zohar. An Early Byzantine Fort in Palestina Tertia. Final Report of Excavations in 1985-1986*, ed. R. P. Harper (Oxford: Oxford University Press), 99–161.

Lernau, O. (2000). "Fish bones," in *Megido III-the 1992-1996 Seasons, Institute of Archeology, Emery and Claire Yass Publication in Archaeology*, eds I. Finkelstein, D. Ussishkin, and B. Halpern (Tel Aviv: Tel-Aviv University), 463–477.

Lernau, O. (2002a). "Fish bones," in *Tel Kabri. The 1986-1993 Excavation Seasons, Institute of Archaeology, Emery and Claire Yass Publications in Archaeology*, ed. A. Kempinski (Tel Aviv: Tel-Aviv University), 409–427.

Lernau, O. (2002b). "Fish remains at Tel Harassim," in *The Sixth Season of Excavation at Tel Harassim (Nahel Barkai) 2000*, ed. S. Givon (Tel Aviv: Tel-Aviv University), 4–13.

Lernau, O. (2008). "The fish bones," in *Neolithic Ashkelon, Qedem Monographs of the Institute of Archaeology*, eds Y. Garfinkel, and D. Dag (Jerusalem: The Hebrew University), 263–268.

Lernau, O. (2009). "Fish Remains," in *Aphek-Anthipatris II, Monograph Series of The Sonia and Marco Nadler Institute of Archaeology*, eds Y. Gadot and E. Yadin (Tel Aviv: Tel-Aviv University), 569–574.

Lernau, O. (2011a). "Fish remains from el-Ahwat," in *El-Ahwat: A Fortified Site from the Early Iron Age Near Nahal 'Iron, Israel. Excavations 1993-2000*, ed. A. Zertal (Leiden: Brill), 362–368. doi: 10.1163/ej.9789004176454.i-488.101

Lernau, O. (2011b). "Fish remains," in *Ashkelon 3: The Seventh Century B.C. (Final Reports of the Leon Levy Expedition to Ashkelon),* eds L. E. Stager, D. M. Master, and J. D. Schloen (Winona Lake, IN: Eisenbrauns).

Lernau, O. (2015). "Fish Bones," in *The Summit of The City of David Excavations 2005-2008. Final Reports Volume I. Area G*, ed. E. Mazar (Jerusalem: Old City Press), 525–538.

Lernau, O., and Golani, D. (2004). "Section B: the osteological remains (aquatic)," in *The Renewed Archaeological excavations at Lachish (1973-1994), Emery and Claire Yass Publications in Archaeology*, ed. D. Ussishkin (Tel Aviv: Tel-Aviv University), 2456–2489.

Leuzinger, L., Kocsis, L., Billon-Bruyat, J.-P., Spezzaferri, S., and Vennemann, T. (2015). Stable isotope study of a new chondrichthyan fauna (Kimmeridgian, Porrentruy, Swiss Jura): an unusual freshwater-influenced isotopic composition for the hybodont shark *Asteracanthus*. *Biogeosciences* 12, 6945–6954. doi: 10.5194/bg-12-6945-2015

Longinelli, A., and Nuti, S. (1973). Revised phosphate–water isotopic temperature scale. *Earth Planet. Sci. Lett.* 19, 373–376. doi: 10.1016/0012-821x(73)90088-5

Luer, C. A., Blum, P. C., and Gilbert, P. W. (1990). Rate of Tooth Replacement in the Nurse Shark, *Ginglymostoma cirratum*. *Copeia* 1990, 182–191. doi: 10.2307/1445834

Luomala, K. (1984). "Sharks and shark fishing in the culture of Gilbert Islands, Micronesia," in *The Fishing Culture of the World: Studies in Ethnology, Cultural Ecology and Folklore,* ed. B. Gunda (Budapest: Akademiai Kiado), 1203–1252.

Martin, E. E., and Scher, H. D. (2004). Preservation of seawater Sr and Nd isotopes in fossil fish teeth: bad news and good news. *Earth Planet. Sci. Lett.* 220, 25–39. doi: 10.1016/s0012-821x(04)00030-5

Mazar, E. (2015). *The Summit of the City of David Excavations 2005-2008. Final Reports Volume I. Area G.* (Jerusalem: Old City Press).

McArthur, J. M., Howarth, R. J., Shields, G. A., and Zhou, Y. (2020). "Chapter 7: Strontium isotope stratigraphy," in *Geologic Time Scale 2020*, Vol. 1, 2, eds F. M. Gradstein, J. G. Ogg, M. D. Schmitz, and G. M. Ogg (Amsterdam: Elsevier), 211–238.

Meredith Smith, M., Underwood, C., Clark, B., Kriwet, J., and Johanson, Z. (2018). Development and evolution of tooth renewal in neoselachian sharks as a model for transformation in chondrichthyan dentitions. *J. Anat.* 232, 891–907. doi: 10.1111/joa.12796

Miake, Y., Aoba, T., Moreno, E. C., Shimoda, S., Prostak, K., and Suga, S. (1991). Ultrastructural studies on crystal growth of enameloid minerals in elasmobranch and teleost fish. *Calcif. Tissue Int.* 48, 204–217. doi: 10.1007/bf02570556

Mokadem, F., Parkinson, I. J., Hathorne, E. C., Anand, P., Allen, J. T., and Burton, K. W. (2015). High precision radiogenic strontium isotope measurements of the modern and glacial ocean: limits on glacial-interglacial variations in continental weathering. *Earth Planet. Sci. Lett.* 415, 111–120. doi: 10.1016/j.epsl.2015.01.036

Moss, S. A. (1967). "Tooth replacement in the lemon shark, *Negaprion brevirostris*," in *Sharks, Skates and Rays*, eds P. W. Gilbert, R. F. Mathewson, and D. P. Rall (Baltimore, MD: Johns Hopkins Press), 319–329.

Nelson, B. K., DeNiro, M. J., Schoeninger, M. J., and De Paolo, D. J. (1986). Effects of diagenesis on strontium, carbon, nitrogen and oxygen concentration and isotopic composition of bone. *Geochim. Cosmochim. Acta* 50, 1941–1949. doi: 10.1016/0016-7037(86)90250-4

Noe-Nygaard, N. (1971). Spur Dog spines from Prehistoric and Early Historic Denmark. *Bull. Geol. Soc. Denmark* 21, 18–33.

Otero, O., Lécuyer, C., Fourel, F., Martineau, H., Mackaye, T., Vignaud, P., et al. (2011). Freshwater fish $\delta^{18}O$ indicates a Messinian change of the precipitation regime in Central Africa. *Geology* 39, 435–438. doi: 10.1130/g31212.1

Pucéat, E., Joachimski, M. M., Bouilloux, A., Monna, F., Bonin, A., Motreuil, S., et al. (2010). Revised phosphate-water fractionation equation reassessing paleotemperatures derived from biogenic apatite. *Earth Planet. Sci. Lett.* 298, 135–142. doi: 10.1016/j.epsl.2010.07.034

Pucéat, E., Lécuyer, C., Sheppard, S. M. F., Dromart, G., Reboulet, S., and Grandjean, P. (2003). Thermal evolution of Cretaceous Tethyan marine waters inferred from oxygen isotope composition of fish tooth enamels. *Paleoceanography* 18:1029

R Core Team (2018). *R: A Language, and Environment for Statistical Computing* Vienna: R Foundation for Statistical Computing.

Raban-Gerstel, N., Bar-Oz, G., Zohar, I., Sharon, I., and Gilboa, A. (2008). Early Iron Age Dor (Israel): a faunal perspective. *Bull. Am. School Orient. Res.* 349, 25–59. doi: 10.1086/basor25067055

Rasch, L., Martin, K., Cooper, R., Metscher, B., Underwood, C., and Fraser, G. (2016). An ancient dental gene set governs development and continuous regeneration of teeth in sharks. *Dev. Biol.* 415, 347–370. doi: 10.1016/j.ydbio.2016.01.038

Reich, R., Shukron, E., and Lernau, O. (2007). Recent discoveries in the City of David, Jerusalem. *Isr. Explor. J.* 57, 153–169.

Reich, R., and Shukron, E. (2011). The date of the Siloam Tunnel reconsidered. *Tel Aviv* 38, 147–157. doi: 10.1179/033443511x13099584885268

Reich, R., Shukron, E., and Lernau, O. (2008). "The Iron Age II Finds from the Rock-Cut 'Pool' near the spring in Jerusalem: A preliminary report," in *Israel in Transition: From Late Bronze II to Iron IIa (c.1250-850 BCE)*, ed. L. L. Grabbe (New York, NY: T&T Clark), 138–143.

Reif, W. E., McGill, D., and Motta, P. (1978). Tooth replacement rates of the sharks *Triakis semifasciata* and *Ginglymostoma cirratum*. *Zool. Jahrb. Abt. Anat. Ontogenie* 99, 151–156.

Reinhardt, E. G., Stanley, D. J., and Patterson, R. T. (1998). Strontium isotopic-paleontological method as a high-resolution paleosalinity tool for lagoonal environments. *Geology* 26, 1003–1006. doi: 10.1130/0091-7613(1998)026<1003:sipmaa>2.3.co;2

Reinhardt, E. G., Stanley, D. J., and Schwarcz, H. P. (2001). Human-induced desalination of Manzala Lagoon, Nile delta, Egypt: evidence from isotopic analysis of benthic invertebrates. *J. Coast. Res.* 17, 431–442.

Retzler, A., Wilson, M. A., and Avni, Y. (2013). Chondrichthyans from the Menuha Formation (Late Cretaceous: Santonian–Early Campanian) of the Makhtesh Ramon region, southern Israel. *Cretac. Res.* 40, 81–89. doi: 10.1016/j.cretres.2012.05.009

Rick, T. C., Erlandson, J. M., Glassow, M. A., and Moss, M. L. (2002). Evaluating the economic significance of sharks, skates, and rays (Elasmobranchs) in prehistoric economies. *J. Archaeol. Sci.* 29, 111–122. doi: 10.1006/jasc.2000.0637

Ripley, B. D. (2002). *Modern Applied Statistics with S*, 4th Edn. (New York, NY: Springer).

Rohling, E. J. (2007). "Oxygen isotope composition of seawater," in *Encyclopedia of Quaternary Science*, Vol. 3, ed. S. A. Elias (Amsterdam: Elsevier), 1748–1756. doi: 10.1016/b0-444-52747-8/00304-5

Rosenfeld, A., and Hirsch, F. (2005). "The Cretaceous of Israel," in *Geological Framework of the Levant: The Levantine Basin and Israel*, Vol. II, eds J. K. Hall, V. A. Krasheninnikov, F. Hirsch, C. Benjamini, A. Flexer (Jerusalem: Historical Productions-Hall), 393–436.

Rosensaft, M., and Sneh, A. (2011). *Geological Map of Israel 1:50,000, Jerusalem Sheet 11-II, State of Israel, Ministry of National Infrastructures, Earth and Marine Research Administration*. Jerusalem: Geological Survey of Israel.

Rowan, Y. M., and Golden, J. (2009). The chalcolithic period of the Southern Levant: a synthetic review. *J. World. Prehist.* 22, 1–92. doi: 10.1007/s10963-009-9016-4

Schilman, B., Bar-Matthews, M., Almogi-Labin, A., and Luz B. (2001). Global climate instability reflected by eastern Mediterranean marine records during the late Holocene. *Palaeogeogr. Palaeoclimatol. Palaeoecol.* 176, 157–176. doi: 10.1016/s0031-0182(01)00336-4

Schmitz, B., Aberg, G., Werdelin, L., Forey, P., and Bendix-Almgreen, S. E. (1991). Sr-87/Sr-86, Na, F, Sr, and La in skeletal fish debris as a measure of the paleosalinity of fossil-fish habitats. *Geol. Soc. Am. Bull.* 103, 786–794. doi: 10.1130/0016-7606(1991)103<0786:ssnfsa>2.3.co;2

Schmitz, B., Ingram, S. L., Dockery, D. T., and Aberg, G. (1997). Testing $^{87}Sr/^{86}Sr$ as a paleosalinity indicator on mixed marine, brackish-water and terrestrial vertebrate skeletal apatite in late Paleocene–early Eocene near-coastal sediments, Mississippi. *Chem. Geol.* 140, 275–287. doi: 10.1016/s0009-2541(97)00023-5

Serena, F. (2005). *Field Identification Guide to the Sharks and Rays of the Mediterranean and Black Sea. FAO Species Identification Guide for Fishery Purposes*. (Rome: FAO), 97.

Sharp, Z. D., Atudorei, V., and Furrer, H. (2000). The effect of diagenesis on oxygen isotope ratios of biogenic phosphates. *Am. J. Sci.* 300, 222–237. doi: 10.2475/ajs.300.3.222

Shaw, H. F., and Wasserburg, G. J. (1985). Sm-Nd in marine carbonates and phosphates: implications for Nd isotopes in seawater and crustal age. *Geochim. Cosmochim. Acta* 49, 503–518. doi: 10.1016/0016-7037(85)90042-0

Shimada, K., and Cicimurri, D. J. (2005). Skeletal anatomy of the Late Cretaceous shark, *Squalicorax* (Neoselachii: Anacoracidae). *PalZ* 79, 241–261. doi: 10.1007/bf02990187

Shimada, K., and Cicimurri, D. J. (2006). "The oldest record of the Late Cretaceous anacoracid shark *Squalicorax pristodontus* (Agassiz), from the Western Interior, with comments on *Squalicorax* phylogeny," in *Late Cretaceous vertebrates from the Western Interior*, eds S. G. Lucas, and R. M. Sullivan (Albuquerque: New Mexico Museum of Natural History and Science), 177–184.

Sisma-Ventura, G., Tütken, T., Peters, S. T. M., Bialik, O. M., Zohar, I., and Pack, A. (2019). Past aquatic environments in the Levant inferred from stable isotope compositions of carbonate and phosphate in fish teeth. *PloS ONE* 14:e0220390. doi: 10.1371/journal.pone.0220390

Sisma-Ventura, G., Tütken, T., Zohar, I., Pack, A., Sivan, D., Lernau, O., et al. (2018). Tooth oxygen isotopes reveal Late Bronze Age origin of Mediterranean fish aquaculture and trade. *Sci. Rep.* 8:14086

Sisma-Ventura, G., Yam, R., Kress, N., and Shemesh, A. (2016). Water column distribution of oxygen and carbon isotopes in the Levantine basin: temporal and vertical change. *J. Mar. Syst.* 158, 13–25. doi: 10.1016/j.jmarsys.2016.01.012

Sisma-Ventura, G., Yam, R., and Shemesh, A. (2014). Recent unprecedented warming and oligothrophy of the Eastern Mediterranean Sea within the last millennium. *Geophys. Res. Lett.* 41, 5158–5166. doi: 10.1002/2014gl060393

Sisma-Ventura, G., Zohar, I., Sarkar, A., Bhattacharyya, K., Zidane, A., Gilboa, A., et al. (2015). Oxygen isotope composition of Sparidae (sea bream) tooth enamel from well-dated archaeological sites as an environmental proxy in the East Mediterranean: a case study from Tel Dor, Israel. *J. Archaeol. Sci.* 64, 46–53. doi: 10.1016/j.jas.2015.10.004

Sivan, D., Greenbaum, N., Cohen-Seffer, R., Sisma-Ventura, G., and Almogi-Labin, A. (2011). The origin and disappearance of the Late Pleistocene – Early Holocene short-lived coastal wetlands along the Carmel coast, Israel. *Quat. Res.* 76, 83–92. doi: 10.1016/j.yqres.2011.04.006

Sivan, D., Sisma-Ventura, G., Greenbaum, N., Bialik, O., Williams, F., Tamisiea, M. E., et al. (2016). Eastern Mediterranean sea levels through the last interglacial from a coastal-marine sequence in northern Israel. *Quat. Sci. Rev.* 141, 204–225. doi: 10.1016/j.quascirev.2016.06.001

Siversson, M., Cook, T. D., Ryan, H. E., Watkins, D. K., Tatarnic, N. J., Downes, P. J., et al. (2018). Anacoracid sharks and calcareous nannofossil stratigraphy of the mid-Cretaceous Gearle Siltstone and Haycock Marl in the lower Murchison River area, Western Australia. *Alcheringa* 43, 85–113. doi: 10.1080/03115518.2018.1462401

Sneh, A., Ram, W., and Eyal, S. (2010). The why, how, and when of the Siloam Tunnel reevaluated. *Bull. Am. Sch. Orient. Res.* 359, 57–65. doi: 10.1086/basor25741828

Starinsky, A., Bielsky, M., Lazar, B., Wakshal, E., and Steinitz, G. (1980). Marine $^{87}Sr/^{86}Sr$ ratios from the Jurassic to Pleistocene: evidence from groundwaters in Israel. *Earth Plant. Sci. Lett.* 47, 75–80. doi: 10.1016/0012-821x(80)90105-3

Staudigel, H., Doyle, P., and Zindler, A. (1985). Sr and Nd isotope systematics in fish teeth. *Earth Planet. Sci. Lett.* 76, 45–56. doi: 10.1016/0012-821x(85)90147-5

Stiller, M., and Magaritz, M. (1974). Carbon-13 enriched carbonate in interstitial waters of Lake Kinneret sediments. *Limnol. Oceanogr.* 19, 849–853. doi: 10.4319/lo.1974.19.5.0849

Suga, S., Taki, Y., and Ogawa, M. (1993). Fluoride and iron concentrations in the enameloid of lower teleostean fish. *J. Dent. Res.* 72, 912–922. doi: 10.1177/00220345930720051301

Talbot, M. R. (1990). A review of the palaeohydrological interpretation of carbon and oxygen isotopic ratios in primary lacustrine carbonates. *Chem. Geol.* 80, 261–279. doi: 10.1016/0168-9622(90)90009-2

Tancioni, L., Mariani, S., Maccaroni, A., Mariani, A., Massa, F., Scardi, M. et al. (2003). Locality-specific variation in the feeding of *Sparus aurata* L.: evidence from two Mediterranean lagoon systems. *Estuar. Coast. Shelf Sci.* 57, 469–474. doi: 10.1016/s0272-7714(02)00376-1

Touzeau, A., Blichert-Toft, J., Amiot, R., Fourel, F., Martineau, F., Cockitt, J., et al. (2013). Egyptian mummies record increasing aridity in the Nile valley from 5500 to 1500 yr before present. *Earth Plant. Sci. Lett.* 375, 92–100. doi: 10.1016/j.epsl.2013.05.014

Toyoda, K., and Tokonami, M. (1990). Diffusion of rare-earth elements in fish teeth from deep-sea sediments. *Nature* 345, 607–609. doi: 10.1038/345607a0

Tuross, N., Behrensmeyer, A. K., and Eanes, D. (1989). Strontium increases and crystallinity changes in taphonomic and archaeological bone. *J. Archaeol. Sci.* 16, 661–672. doi: 10.1016/0305-4403(89)90030-7

Tütken, T., Vennemann, T. W., Janz, H., and Heizmann, H. E. P. (2006). Palaeoenvironment and palaeoclimate of the Middle Miocene lake in the Steinheim basin, SW Germany: A reconstruction from C, O, and Sr isotopes of fossil remains. *Palaeogeogr. Palaeoclimatol. Palaeoecol.* 241, 457–491. doi: 10.1016/j.palaeo.2006.04.007

Tütken, T., Vennemann, T. W., and Pfretzschner, H.-U. (2008). Early diagenesis of bone and tooth apatite in fluvial and marine settings: constraints from combined oxygen isotope, nitrogen and REE analysis. *Palaeogeogr. Palaeoclimatol. Palaeoecol.* 266, 254–268. doi: 10.1016/j.palaeo.2008.03.037

Tütken, T., Vennemann, T. W., and Pfretzschner, H.-U. (2011). Nd and Sr isotope compositions in modern and fossil bones - proxies for vertebrate provenance and taphonomy. *Geochim. Cosmochim. Acta* 75, 5951–5970. doi: 10.1016/j.gca.2011.07.024

Underwood, C., Johanson, Z., and Smith, M. M. (2016). Cutting blade dentitions in squaliform sharks form by modification of inherited alternate tooth ordering patterns. *R. Soc. Open Sci.* 3:160385. doi: 10.1098/rsos.160385

Van den Brink, E. C. M., Barzilai, O., Vardi, J., Cohen Weinberger, A., Lernau, O., Liphschitz, N., et al. (2016). Late Chalcolithic settlement remains East of Namir Road, Tel Aviv. *J. Isr. Prehist. Soc.* 46, 20–121.

Van Neer, W., Ervynck, A., and Monsieur, P. (2015). Fish bones and amphorae: evidence for the production and consumption of salted fish products outside the Mediterranean region. *J. Rom. Archaeol.* 23, 161–195. doi: 10.1017/s104775940000235x

Van Neer, W., Lernau, O., Friedman, R., Mumford, G., Poblome, J., and Waelkens, M. (2004). Fish remains from archaeological sites as indicators of former trade connections in the Eastern Mediterranean. *Paléorient* 30, 101–148. doi: 10.3406/paleo.2004.4775

Van Neer, W., Zohar, I., and Lernau, O. (2005). The emergence of fishing communities in the eastern Mediterranean region: a survey of evidence from pre- and protohistoric periods. *Paléorient* 31, 131–157. doi: 10.3406/paleo.2005.4793

Van Neer, W., De Cupere, B., and Waelkens, M. (1997). "Remains of local and imported fish at the ancient site of Sagalassos (Burder Prov. Turkey)," in *Sagalassos IV: Report on the Survey and Excavation Campaigns of 1994 and 1995*, eds M. Waelkens, and J. Poblome (Leuven: Leuven University Press), 571–586.

Van Neer, W., and Depraetere, D. (2005). Pickled fish from the Egyptian Nile: osteological evidence from a Byzantine (Coptic) context at Shanhûr. *Rev. Paléobiol.* 25, 159–170.

Van Neer, W., and Ervynck, A. (2004). "Remains of traded fish in archaeological sites: indicators of status, or bulk food?" in *Behaviour Behind Bones: The Zooarchaeology of Ritual, Religion, Status and Identity*, eds S. J. O'Day, W. Van Neer, and A. Ervynck (Oxford: Oxbow Books), 203–214.

Vengosh, A., Sprivack, A. J., Artzi, Y., and Ayalón, A. (1999). Geochemical and boron, strontium, and oxygen isotopic constraints on the origin of the salinity in groundwater from the Mediterranean coast of Israel. *Water Resour. Res.* 35, 1877–1894. doi: 10.1029/1999wr900024

Vennemann, T. W., Fricke, H. C., Blake, R. E., O'Neil, J. R., and Colman, A. (2002). Oxygen isotope analysis of phosphates: a comparison of techniques for analysis of Ag_3PO_4. *Chem. Geol.* 185, 321–336. doi: 10.1016/S0009-2541(01)00413-2

Vennemann, T. W., and Hegner, E. (1998). Oxygen, strontium, and neodymium isotope composition of fossil shark teeth as a proxy for the palaeoceanography and palaeoclimatology of the Miocene northern Alpine Paratethys. *Palaeogeogr. Palaeoclimatol. Palaeoecol.* 142, 107–121. doi: 10.1016/s0031-0182(98)00062-5

Vennemann, T. W., Hegner, E., Cliff, G., and Benz, G. W. (2001). Isotopic composition of recent shark teeth as a proxy for environmental conditions. *Geochim. Cosmochim. Acta* 65, 1583–1599. doi: 10.1016/s0016-7037(00)00629-3

Wacker, U., Rutz, T., Löffler, N., Conrad, A. C., Tütken, T., Böttcher, M. E., et al. (2016). Clumped isotope thermometry of carbonate-bearing apatite: revised sample pre-treatment, acid digestion, and temperature calibration. *Chem. Geol.* 443, 97–110. doi: 10.1016/j.chemgeo.2016.09.009

Weber, M., Lugli, F., Jochum, K. P., Cipriani, A., and Scholz, D. (2018). Calcium Carbonate and Phosphate Reference Materials for Monitoring Bulk and Microanalytical Determination of Sr Isotopes. *Geostand. Geoanal. Res.* 42, 77–89. doi: 10.1111/ggr.12191

Weber, M., Wassenburg, J. A., Jochum, K. P., Breitenbach, S. F. M., Oster, J., and Scholz, D. (2017). Sr-isotope analysis of speleothems by LA-MC-ICP-MS: high temporal resolution and fast data acquisition. *Chem. Geol.* 468, 63–74. doi: 10.1016/j.chemgeo.2017.08.012

Wheeler, A., and Jones, A. K. G. (1989). *Fishes*. (Cambridge: Cambridge University Press).

Wilson, M. A., Zatoń, M., and Avni, Y. (2012). Origin, palaeoecology and stratigraphic significance of bored and encrusted concretions from the Upper Cretaceous (Santonian) of southern Israel. *Palaeobiodiv. Palaeoenviron.* 92, 343–352. doi: 10.1007/s12549-012-0082-8

Woodward, J. C., Macklin, M. G., Fielding, L., Millar, I., Spencer, N., Welsby, D., et al. (2015). Shifting sediment sources in the world's longest river: a strontium isotope record for the Holocene Nile. *Quat. Sci. Rev.* 130, 124–140. doi: 10.1016/j.quascirev.2015.10.040

Zacke, A., Voigt, S., Joachimski, M., Gale, A., Ward, D., and Tütken, T. (2009). Surface-water freshening and high-latitude river discharge in the Eocene North Sea. *J. Geol. Soc.* 166, 969–980. doi: 10.1144/0016-76492008-068

Zohar, I. (2017). "Fish exploitation during the Quaternary: recent knowledge," in *Quaternary of the Levant: Environments, Climate Change, and Humans*, eds Y. Enzel and O. Bar-Yosef (Cambridge: Cambridge University Press), 369–376. doi: 10.1017/9781316106754.043

Zohar, I., and Artzy, M. (2019). The role of preserved fish: evidence of fish exploitation, processing, and long-term preservation at the Eastern Mediterranean, during the Late Bronze Age (14th-13th centuries BCE). *J. Archaeol. Sci. Rep.* 23, 900–909. doi: 10.1016/j.jasrep.2018.12.008

Zohar, I., and Biton, R. (2011). Land, lake, and fish: investigation of fish remains from Gesher Benot Ya'aqov (paleo-Lake Hula). *J. Hum. Evol.* 60, 343–356. doi: 10.1016/j.jhevol.2010.10.007

Zohar, I., Dayan, T., Spanier, E., Galili, E., and Lernau, O. (1994). Exploitation of gray triggerfish (*Balistes carolinensis*) by the prehistoric inhabitants of Atlit-Yam, Israel: a preliminary report, in *Fish Exploitation in The Past: Proceedings of the 7th meeting of the ICAZ Fish Remains Working Group*, ed. W. Van Neer (Tervuren: Musée Royal de l'Afrique Centrale), 231–237.

Zohary, T., Erez, J., Gophen, M., Berman-Frank, I., and Stiller, M. (1994). Seasonality of stable carbon isotopes within the pelagic food web of Lake Kinneret. *Limnol. Oceanogr.* 39, 1030–1043. doi: 10.4319/lo.1994.39.5.1030

Conflict of Interest: The authors declare that the research was conducted in the absence of any commercial or financial relationships that could be construed as a potential conflict of interest.